UCL Université catholique de Louvain

École polytechnique de Louvain (EPL)

epl

Musculoskeletal modelling of the bird

Dissertation presented by
Guillaume LAMINE

for obtaining the Master's degree in
Electro-mechanical Engineering
Option(s): Mechatronics

Supervisor(s)
Renaud RONSSE

Reader(s)
Philippe CHATELAIN, Julien HENDRICKX , Victor COLOGNESI

Academic year 2017-2018

Abstract

Nowadays, there are already multiple ways that the birds have been studied. Turbulence effects on the aerodynamic point of view, as well as their scaling in zoology. However, this paper has the particularity to gather the notions from different topics in order to simulate the flight of the bird. The analysis goes from the development of mechanical multibody model and the scaling of all its parameters, to a bio-inspired actuation of all the wing beat. In order to do this, an aerodynamic model has been added to the mechanical one, and the kinematics of flight have been studied from data measures coming from the Geronticus Eremita, which is the bird of interest. This project is part of the larger one, called RevealFlight whose purpose is to understand the link between muscle activation patterns and kinematics of flight, and later, the interactions in flock of birds.

Acknowledgements

I am deeply grateful for all the work achieved through the realization of this Master thesis. I am convinced that the result will allow others to build on that first step and continue on the project RevealFlight which is still full of opportunities. I am grateful for the discoveries and lessons I made and encountered and I know that this knowledge will continue to rise in the future, and in what life can bring of wonderful.

I especially wanted to thanks **Prof. Renaud Ronsse**, for his support as my supervisor. His good advices made me find the right path. In times where I was diverging, lost in the amount of information, he helped me to focus to the important.

I also wanted to thanks **Victor Colognesi** for his help in the implementation of the aerodynamic model. As he was working on the project of RevealFlight, some good infortions were transmitted. There is the help of **François Heremans**, that I wanted to mention for his insights concerning the modelling of the muscles of the bird.

Finally, nothing of this work would have been possible if I had not been supported morally by all the people around me. Thank you very much to my parents, brother and sisters, as well as the friends who gave me feedbacks on all these simulations, schematics and analysis.

Guillaume Lamine Wavre, August 2018

List of abbreviations

General abbreviations

DOF	Degree Of Freedom
EMG	Electromyography

Structural dimensions

HumL	Humerus Length
UlnL	Ulna Length
CMCL	Carpometacarpus Length
FprimL	Primary Feather Length
ICS	Inter-coracoid Space

Muscles names

Shoulder muscles

PT	Pectoralis muscle
PTclav	Pectoralis msucle - clavicle part
SC	Supracoracoideus muscle
SHC	Scapulohumeralis Caudalis muscle

Wing morphing muscles

TH	Triceps Brachii Humeral head
BB	Biceps Brachii
ECU	Extensor Carpi Ulnaris
FCU	Flexor Carpi Ulnaris
EMR	Extensor Metacarpi Radialis
TP	Tensor Propatagialis

Contents

Chapter 1

Introduction

1 Project objectives

This project is part of the RevealFlight Project.[1]

« The RevealFlight project aims at shedding light on the efficiency optimization mechanisms deployed by biological flyers. We will focus on birds, and in particular on migratory birds, which are known to exhibit such efficiency-seeking mechanisms at several levels, while maintaining relatively stable flight conditions, leading to impressive results. »

The current thesis is the first step of RevealFlight, even though all the aspects of the complete objective of RevealFlight are not already implemented. Here, the research is mainly oriented towards the development of the multi-body mechanical system of a bird itself. Afterwards, a first temporary aerodynamic model is implemented in order to already allow the bird to fly alone. All the dimensions of the bird model will have to be scaled to the bird of interest of the thesis which is the Geronticus Eremita, also called Bald Ibis (See Figures 1.1 and 1.2). In this thesis, we will only focus on a steady state level flight with constant height and speed. Next, there will be an extensive analysis of the kinematics of the flight of the Geronticus Eremita.

The muscles model will already be implemented. However, in order to actuate the muscles, one need the patterns of activation. For now, these patterns can be seen as equivalent to the signals of Electromyography (EMG) that can be recorded on birds. As the link between EMG signals and kinematics has never been highlighted, the purpose of this thesis is to inverse the dynamical model and muscle models in order to, for the first time, link kinematics of flight, equivalent mechanical torques in the joints and muscles activation patterns.

Nevertheless, a few steps are necessary to obtain the muscle models and invert them. Firstly, the right equivalent muscle must be chosen from real flight muscles, as well as their attachments points. The more these dimensions are precise, the more chances it has to give similar activation as the ones measured from EMG. Secondly, the parameters of the muscle models, which are numerous, need to be approximated. Thirdly, a resolution of the over-actuation generally encountered in reality in bio-mechanical muscle systems will be provided.

[1] https://sites.uclouvain.be/RevealFlight/

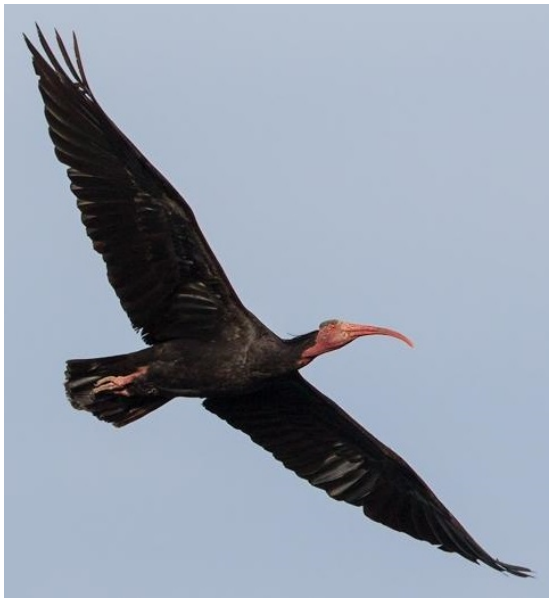

Figure 1.1 – Geronticus Eremita in gliding flight.

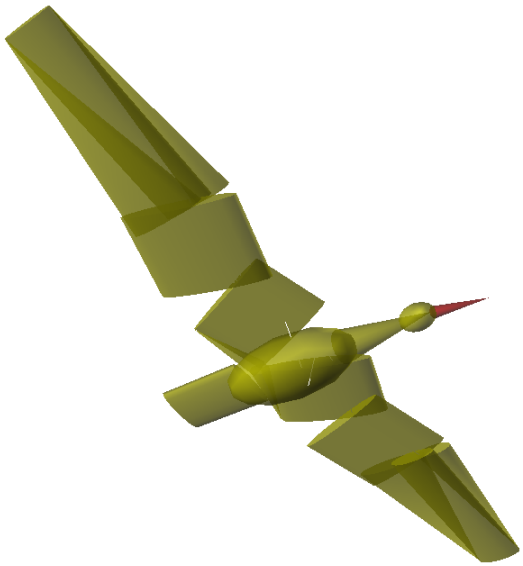

Figure 1.2 – Robotran model equivalent of the Geronticus Eremita.

2 State of the art

The state of the art in the special topic of musculoskeletal modelling of a bird is a quite restraint area. However, multiple research have already been done in the separate sub-topics that the thesis is gathering. Therefore, state of the art can be covered for the different sub-topics.

Multiple types of mechanical models of birds have already been implemented. Many of them are used in the computer graphics area [10] [22] in order to produce realistic reproduction of birds in games and movies. However, the model developed here has taken more of a bio-mechanical approach based on anatomy. This approach is typically not the one chosen by computer graphics.

There are also in the literature models developed to apply optimization processes [14] [15]. Their approach is generally based on evolutionary algorithms which means that data from the bird itself is not the starting point.

Aerodynamics models in the analysis of bird flight are also multiple and of variable complexity in the literature. Each of them has different purposes. There are the ones using precise computational-fluid with an interest oriented towards precise analysis of wake and turbulence, created by the wings. RevealFlight will tend towards this objective, but it is not the approach of the current thesis. There are also models modelling separately all feathers and applying the equations of Lift and Drag on each segment. The approach chosen in this thesis is similar. The aerodynamic model is also based the equations of Lift and Drag even though the feathers are not yet represented separately. Instead, the wing are cut in segments where the model is applied.

Scaling of the birds has already been studied by many biologists, but rarely by engineers. This approach allows to link all the literature available in biology and the mechanical simulations available in engineering. The search for patterns of isometry and allometry done by Pennycuick [13], Simons [16], Field [6] and Wang [20], among others, and their gathering of data set has allowed to extrapolate dimensions of the Geronticus Eremita. In the frame of the modelling of flying birds, the scaling is generally not a center question. Much more interest will be dedicated to the scaling in this thesis.

Concerning kinematics, the more precise data are all coming from the research done by biologists. However, like in [10], large data sets have also been recorded in order to simulate the flight of the bird. Nevertheless, this large data sets are used only with artificial neural networks that are able to identify the patterns of flight. Our approach in this thesis is more analytical.

Given the few recordings of data at hand during the thesis, the measures are here decomposed and approximated by analytical functions.

The modelling of muscles with Hill models is encountered multiple times in the literature. These models can be seen, among other areas, in bio-inspired humanoid gait modelling [8] [18]. However, it has never been used on bird models. This is a special characteristic of the thesis that will allow to make for the first time a link between real muscles recordings of data and real kinematics observed in flying birds. It will serve of confirmation step. Indeed, multiple authors have recorded data of bird flight and muscles stress and strain [3].

3 Reading guide

Chapter 2 : Multi-body mechanical model of the bird

The Chapter 2 begins the thesis with the creation of the multi-body mechanical system of the birds. The Degrees of Freedom (DOF) will have to be carefully chosen and the choices will imply multiple assumptions. The choices will me motivated by other models of the literature as well as analysis by other author of the wings possible movement during the wing beat. At this stage the bird model is still general and has no quantified values within. Afterwards, a small description of the environment of simulation, the Robotran software, is covered.

Chapter 3 : Aerodynamic model for flying

In Chapter 3, the multi-body mechanical system is completed with an aerodynamic model. The aerodynamic equations are applied to the segments of the wings. This feature will allow the bird to fly, once the wings kinematics are identified. Kinematics will be studied in Chapter 5. In order to have a working aerodynamic model, the wing profiles must defined adn that will also be the purpose of the Chapter. However, all dimensions are still unknown, leaving the model as a parametric model. Once again, all the assumptions done during the modelling and implications on the results will be covered.

Chapter 4 : Scaling of the bird - Parameters identification

Now that the bird is modelled like a full parametric model, one need to identify the parameters. This is the focus of Chapter 4. As a reminder, the bird of interest is the Geronticus Eremita. As there are no data available for the bird, the only solution is to extrapolate the data from other birds. This Chapter explains how it can be done, thanks to patterns of isometry and allometry among bird species and taxa. This parameters identification will allow to complete the mechanical and aerodynamic model. In the end, has the ability to fly. Given the right kinematics, it should fly similarly to the bird studied.

Chapter 5 : Kinematic analysis of the flight

All the necessary values have been gathered and now the bird is ready to fly. However, the bird does not know yet how to fly. First, it is needed to understand the way of flying of the Geronticus Eremita in order to implement it in the simulator and make the model fly. This is done through the analysis of kinematic data from a Geronticus Eremita in steady speed and height flight. This is called a level flight. From this data, multiple approximation are done to write down the kinematics in forms of analytical functions. Finally, the result is compared to data from other birds in the literature and also plotted against the data set of approximation, to evaluate the errors of approximations.

Chapter 6 : Actuation by muscle modelling

The bird flies as wanted in the case of a level flight. In this Chapter, a new component is added to the model. This is the muscle models. The purpose of these models is to actuate the bird model with bio-inspired controllers. In fact, until now, the bird is constrained kinematically to achieve the wanted pattern of wing beat. The goal is then to replace the constraints by muscles. Firstly, all existing flight muscles of the bird are covered and some among them are chosen to make the movement possible. Muscle models take as input the instantaneous state of the bird and also activation patterns, similar to EMG signals and outputs a force. Because these signals are unknown, this thesis will limit to the inversion of the mechanical model. Given the equivalent torques in the joints, it will be possible to invert the muscle models. The ideal goal would be to obtain the activation patterns. To achieve this, muscle parameters must be found for each muscle as well as all their attachment points.

Chapter 7 : Conclusion - Take-aways and perspectives

The last Chapter summarizes the entire reasoning and the results obtained as well as the work achieved until here. It will necessarily speak about the limitations of the different aspects of the thesis. Knowing the limitations it will then be possible to have a better insight of the future perspectives of the project. As the project is the first step of RevealFlight, it will be interesting to highlight the next steps to come.

Chapter 2

Multi-body mechanical model of a bird

This Chapter is dedicated to the elaboration of general parametrized mechanical model of a bird. Thus, this model should be valid for any bird. It is only further in Chapter 4 that these parameters will be adapted to the Geronticus Eremita, the bird of focus. First of all, all the Degrees Of Freedom (DOF) will be justified along with all the assumptions made. The chosen sub-bodies of the mechanical system will be enumerated. Afterwards, the software environment used to simulated the mechanical system will be introduced. It will allow a better insight on the parameters of interest.

1 Description of the model - degrees of freedom

As a reminder, the goal of the thesis is to elaborate a mechanical model which most closely reflects reality. However, a few assumptions are needed to model a system as complex as a bird.

The full bird system with all sub bodies can be visualized as the ones of Figure 2.2. Obviously, the system needs to be simplified. As the purpose of the model is to make a bird fly in steady state at constant speed and constant height, all the bones not directly involved are not modelled.

Moreover, an important element to highlight is that in this study, the only DOF allowed to the main body of the bird are 2 DOF out of the 6 possible. The bird is constrained on each of the three rotation axis. For now, the bird can not roll, pitch or yaw. The final constraint is that the bird can not translate along the pitch axis. These constraints could be relaxed later. It leaves only translations on the roll and yaw axis. Those are of main interest as the goal is to model a flight in straight line in constant speed, and generate enough lift to compensate gravity.

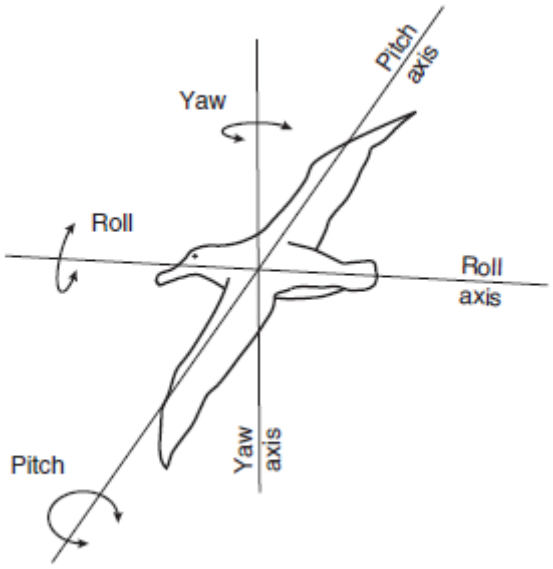

Figure 2.1 – General axis of rotation roll, pitch and yaw defined for a flying bird. (Figure taken from Pennycuick [13])

Here are the simplifications and assumptions made :

1. The tail of the bird is not modelled. It is assumed to be mainly of directional use and negligible in the lift force on the bird, compared to the one produced by the wings.
2. The legs are not modelled and considered to have no influence on a steady state flight. (Note that they are essential for taking off, and need to be added if one wants to model the take off)
3. No movements of the head are taken into account
4. The scapula, coracoid and furcula are considered to be fixed.
5. The digits of the wings are not modelled.

These simplifications leave the model as two wings fixed to only one main body that has only 2 DOF. Concerning the wings : they are composed of the following bones, the humerus, ulna, radius, carpometacarpus, three digits with a total of five phalanx, and two ossicles, the radiale and ulnare.

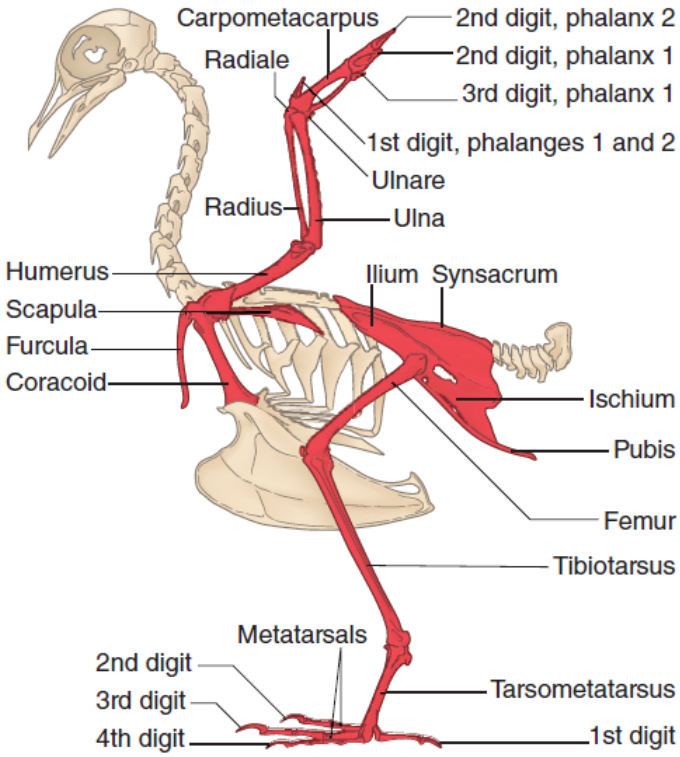

Figure 2.2 – Schematic of the skeleton of a bird. The limbs shaded in red is the appendicular skeleton. Those are the limbs that supports movements associated with flying, swimming, running and jumping. (Figure taken from Cornell Lab of Ornithology's handbook [12])

Before further simplify, it is needed to have a deeper understanding of the DOF needed in a wing for bird flight. The assumption from [1] is taken : much of the active wing morphing actuated by the muscles, in soaring, gliding or flapping flight can be described by three kinematic variables : wing folding or expanding, wing twisting, and wrist flexing or extending (Figure 2.3).

To be able to achieve the folding and expanding, 1 DOF in rotation is needed in the shoulder, elbow and wrist joint. Twisting is achieved thanks to the ulna and radius rotation around each other. To simplify the arm, the ulna and radius are replaced by one unique body, that has 1 DOF at the elbow. This allows the modelling of the twisting. Finally, the wrist can be flexed and extended just by adding a second rotation DOF on the wrist.

Next to those, like a human shoulder, two more DOF can be added to the shoulder of the bird : One DOF for the beating and one DOF for the general orientation of the wing relative to the main body. It makes 7 DOF for each wing and a total 16 DOF for the whole system. This choice of DOF is partially inspired from [22] and [10].

(a) Wing folding or expanding - 3 rotation DOF constrainted kinematically by 2 Equations to achieve 1 movement

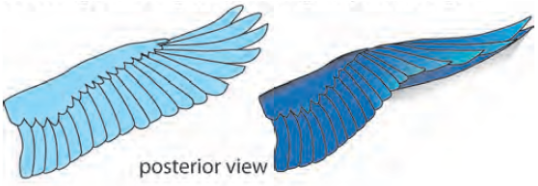

(b) Wing twisting (supinating or pronating) - 1 DOF

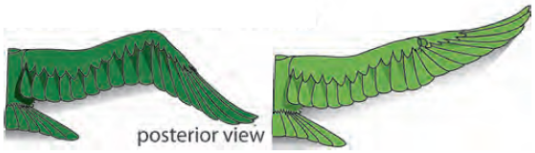

(c) Wing flexing or extending - 1 DOF

Figure 2.3 – The fbird flight can be approximated by a composition of three movement : folding 2.3a, twisting 2.3b and flexing 2.3c. It is equivalent to a total of 5 DOF. By adding the beating and general orientation of the wing, it makes a total of 7 DOF for a whole bird wing. (Figure taken from Altshuler et al [1])

In this section, the mechanical model of the bird of interest will be described. The purpose here is to obtain a model that is as close to reality as possible. The final choice for the modelling is to give 7 degrees of freedom to each wing. It is done the same in the literature in [22] and [10]. Moreover, as explained in [1], the flight of the bird can be parametrized with a composition of the three movements of the Figure 2.3.

In this Figure, 2.3a need 3 DOF, 2.3b need 1 DOF and 2.3c 1 DOF.

Added to that, there is the DOF needed for the beating of the wing and a last one, to allow the whole movement of the wing to rotated with respect to the body of the bird. It is indeed a total of 7 DOF for one wing.

For now, the body of the bird is only allowed 2 DOF of translation, to simplify our approach. It makes a total of 16 DOF for the whole bird.

The degrees of freedom are defined in the following way :

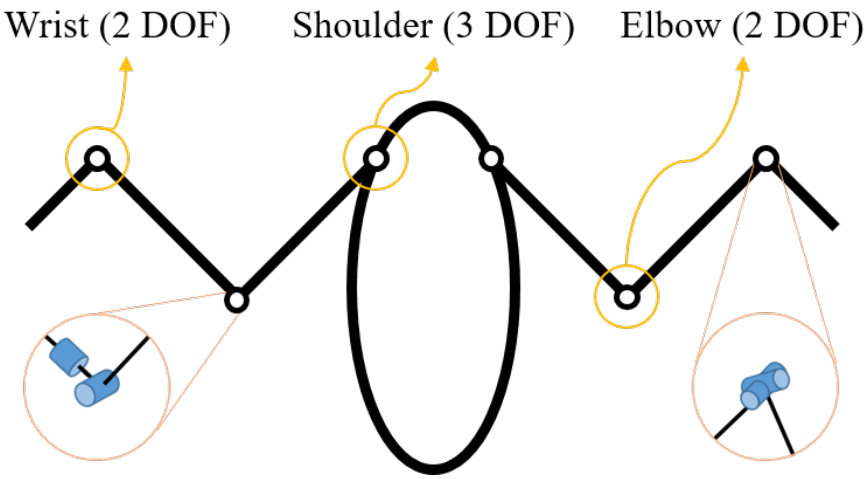

Figure 2.4 – The complete bird model is composed of 16 DOF : shoulders have 3 rotation DOF each, equivalent to spherical joints; elbows have 2 DOF, one for folding the elbow (Rotation axis perpendicular to the bones bodies) and one for twisting it (Long axis rotation); wrists have 2 rotation DOF by a combination of 2 revolute joints.

2 Simulation tool - Robotran model

Now that the general model is fixed, it can be built in a simulator in order to proceed with the simulations. The software environment used is Robotran. It is a multibody dynamics simulator, using Newton-Euler symbolic generation of the equations of motion. Even tough it is initially made for rigid bodies, it can easily be coupled with an aerodynamic model or muscles model for the actuation, as it will be done in later Chapters.

The current mechanical model in Robotran at this level is shown on Figure 2.5. As explained in Section 1, `Bird_body` has 2 DOF, `LowerArm_R` and `LowerArm_L` have the 3 DOF at the shoulder, `UpperArm_R` and `UpperArm_L` have the 2 DOF at the elbow and `Hand_R` and `Hand_L` have 2 DOF at the wrist.

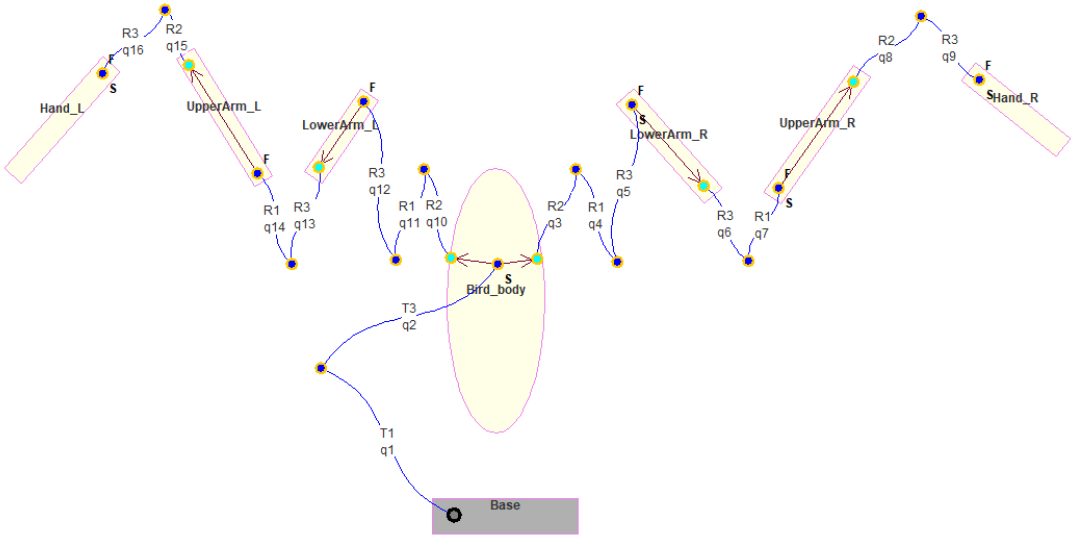

Figure 2.5 – The Figure represent the current Robotran model. It is composed of 7 bodies and 16 DOF. $R1$, $R2$, $R3$ and $T1$, $T2$, $T3$ respectively define rotation around x-, y- and z-axis and translation along x-, y- and z-axis. (More informations on website `http://www.robotran.be/`

In Figure 2.5, $R1$, $R2$, $R3$, are respectively rotation DOF around x-, y- and z-axis and $T1$, $T3$, translations along x- and z-axis.

As it can be seen on the model representation, Robotran needs all the lengths between the fixation points of the joints. The reference frame on the bird is defined as aligned with the base frame, and the origin placed in the middle of the line linking the two shoulder's joints. Moreover, Robotran also needs all the masses and inertia matrices of the bodies. Finding these values is the objective of Chapter 4.

Chapter 3

Aerodynamic model for flying

This Chapter covers all the aerodynamic components of the bird model. First, the model used is presented in a general sense with some simple aerodynamic definitions. Afterwards, it will be shown how to complete the model parameters from the values obtained in Chapter 4.

1 The aerodynamic model

The aerodynamic model is based on the Equations 3.1 and 3.2 for Lift and Drag. Theses equations are to be applied on each wing. Moreover, each wing is cut in three segments. Thus, the wing is approximated by three segments of ideal wings.

The purpose of this Chapter is to present the current aerodynamic model chosen to allow the bird to fly. The method is the same as in [22] and [10]. The principle is to mainly use the aerodynamic equations of lift and drag forces. These notions are defined on Figure 3.1. The angle of attack is the coefficients of lift and drag, respectively $C_L(\alpha)$ and $C_D(\alpha)$.

Lift and Drag forces are expressed as follows:

$$Lift = \frac{1}{2} C_L(\alpha) \rho V^2 S[N] \tag{3.1}$$

$$Drag = \frac{1}{2} C_D(\alpha) \rho V^2 S[N] \tag{3.2}$$

First of all, Lift and Drag force vectors are defined respectively as perpendicular and parallel to the relative wind. The forces are applied on the line of pressure. In the equations, V is the amplitude of the vector of relative wind. Note that this vector is projected in the plane of the chord line and is perpendicular to the pressure line. S is the surface of the wing. It is a scalar value. Finally, ρ is the mass density of the fluid, which is air in this case.

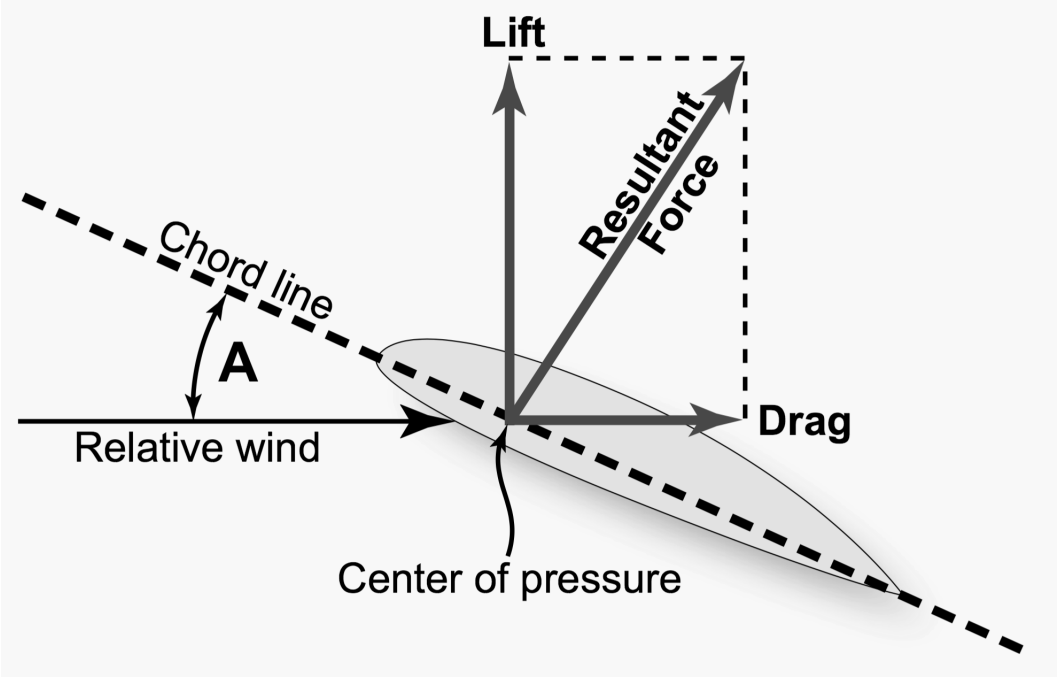

Figure 3.1 – Definition of the aerodynamic notions

This model is directly inspired from airplanes. However, unlike the rigid wing of a plane, the bird here has multiple degrees of freedom in its wing. Therefore, the choice has been made to cut the bird wing into three portions that can move relatively to each other. In practice, the wing model is equivalent to three rigid plates. It is important to realize that the model is not representing the flexible characteristics of the feathers. Moreover, when the bird is folding its wings, the equivalent wing surface is still constant in the model. The only influence of folding is to change the relative air flow vector, which helps to diminish the lift and drag.

Also, this model is not taking into account turbulence, vortex and wakes effects. Nevertheless, multiple studies have already shown that birds are using these effects to fly.

2 Parameters of the model

After choosing the model, a few parameters are still to be defined. In Robotran, the three portions are defined as trapezoidal forms. The profile is assumed to be perpendicular to the bones of the wing. The four unknown lengths of the three trapezes are taken from a picture of a Geronticus Eremita in flight. Still, the real measure is unknown. The four length must be multiplied by a proportionality factor. To find this factor α, the model is imposed to have an equal Wing Area, as previoulsy found in the Chapter on scaling.

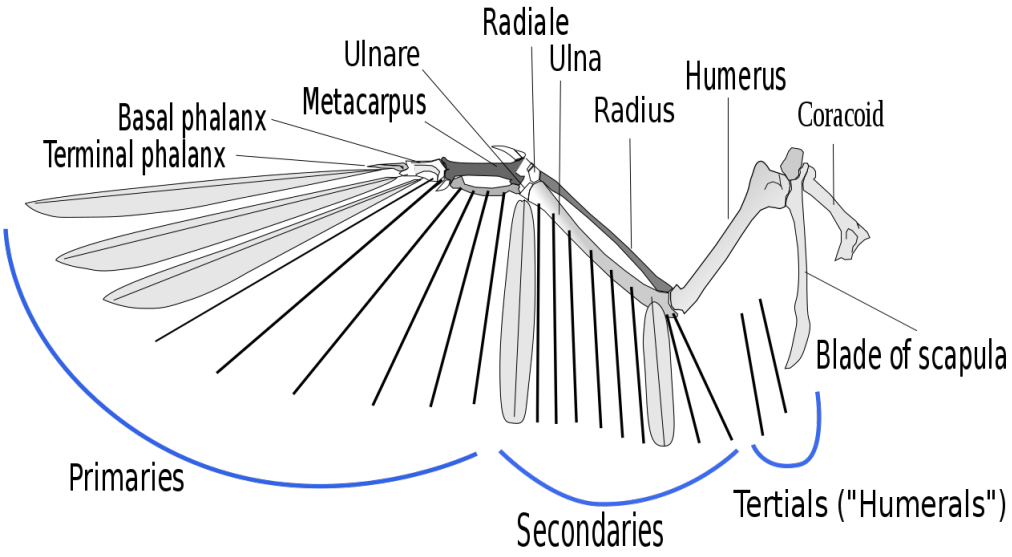

Figure 3.2 – The bird wing has three types of feathers to generate lift forces : primaries, secondaries and tertials. Most of lift is produced by the secondaries and most of the thrust by the primaries. Primaries all originate on the carpometacarpus and phalanxes and secondaries on the ulna. In practice, a bird is never completely extending the elbow. A muscle called Tensor Propatagialis connects shoulder and wrist to keep a straighter edge during flight. (More details in Chapter 6)(Figure taken from https://en.wikipedia.org/wiki/Flight_feather)

Concerning the lengths of the trapezes, the bones are assumed to be close to aligned in a straight line. It is not the case as visible on Figure 3.2. For the sections of humerus and ulna, the lengths are then directly the lengths of the bones. For the Carpometacarpus, the full length is considered to be CMCL added to the length of a primary feather. In other words, the last segment is assumed to be the continuity of the hand and a primary feather aligned. It seems accurate as, anatomically, the latest primary feather is positioned at the tip of phalanx 2 of the second digit. The obtained values are : $x = 0.134\ [m]$ $y = 0.162\ [m]$ and $z = 0.349\ [m]$.

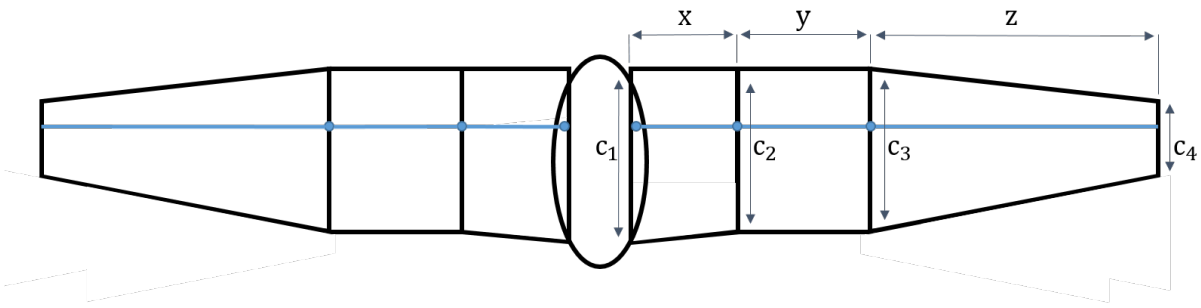

Figure 3.3 – Idealized profile of the bird wings in the model. The three segments are assumed to be aligned : all humerus, ulna and carpometacarpus are on a straight line. It means that x y z are respectively the lengths of the humerus, ulna and carpometacarpus plus primary feather together. c_1, c_2, c_3 and c_4 are the chords of the profile at the limits of the trapezoidal sections. The chords are placed at $\frac{1}{4}$ of their length on the bone line with the longer $\frac{3}{4}$ part away from the leading edge of the profile.

Thanks to the values of wing span and wing area, added to some useful pictures of Geronticus Eremita, the dimensions on Figure 3.3 have been chosen for the wing model. It is possible to visually compare them on Figure 3.4.

Finally, the four chords for the trapezoidal forms are : $c_1 = 0.218$ $[m]$, $c_2 = c_3 = 0.2$ $[m]$ and $c_4 = 0.091$ $[m]$ and a proportional factor $\alpha = 0.0181416$

Something to be noticed is that the model is an idealized version as well as an approximation. In practice, it would make more sense to cut the wing by section of feathers. However, the current model can not take this into account as segments are trapezoidal and perpendicular to the bone. This is not the case of the feathers, as it can be seen on Figure 3.2.

(a) (b)

Figure 3.4 – (a) : Geronticus Eremita in gliding flight; (b) : Robotran equivalent of the Geronticus Eremita. (Figure taken from https://www.hbw.com/ibc/photo/northern-bald-ibis-geronticus-eremita/adulte-bird-flying-over-coast)

Concerning the aerodynamic values : the mass density of the air is chosen to $\rho = 1.225$ $[\frac{kg}{m^3}]$. The coefficients of lift and drag are taken from a general model of symmetric streamlined profile of wing, similar to the one of Figure 3.1. The assumption is made that for large birds, such profile is a good approximation. Their value, which depends on the angle of attack, are shown at Figure 3.5.

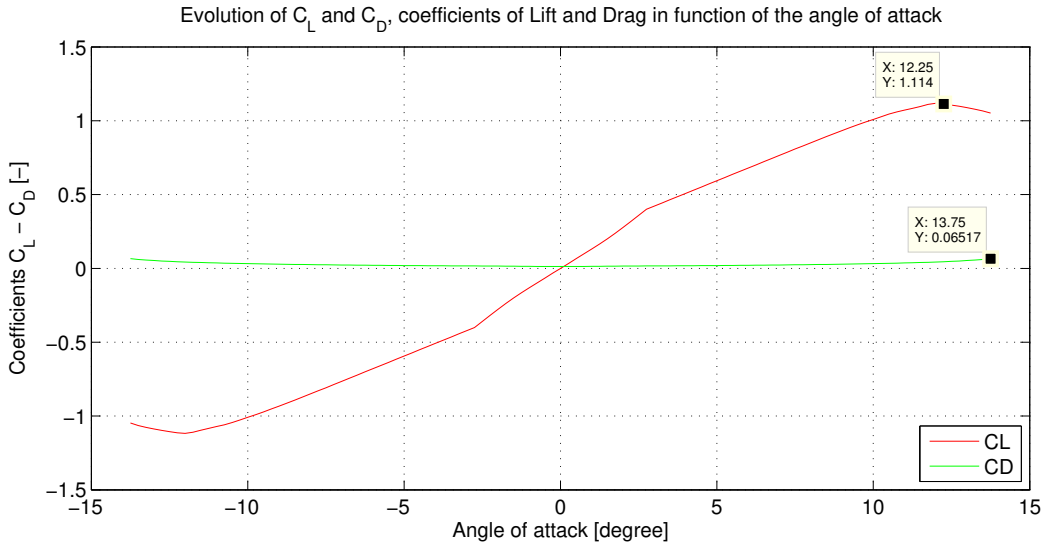

Figure 3.5 – Data values of the coefficients of lift and drag used in the aerodynamic model of the bird. Stalling angle is about 12.25°. For the simulations, outside these boundaries, the coefficients are considered to stay constant.

It is interesting to note on Figure 3.5 that the lift coefficient reaches a maximum when angle of attack is 12.25°. It means that beyond this angle, the wing is stalling. In the case of this study, the interest is only focused on steady speed and constant height flight. For the analysis, the angle of attack should stay inside those borders. However, for more particular situations such as maneuvering, the angle of attack could get outside the bounds. In this case, a more complex model would probably be useful.

3 Implementation in Robotran

The Robotran software allows to couple the initial multi-body system of rigid bodies with the aerodynamic model detailed above. An aerodynamic bloc coded in MATLAB (MathWorks 2014) and coupled to Robotran helps compute the aerodynamic forces. The possible forces to apply to the system are Joint Forces or External Forces. The most appropriate here will be the external ones. In practice, each of the three sections of each wing need to be discretized. It is here done by slices of 2.5 $[cm]$. Moreover, the general aerodynamic code is defined in a default referential. It is necessary to express the forces in the inertial coordinate frame for each of the six sections. Robotran gives easy access to all the rotation matrices of the multi-body system.

Chapter 4

Scaling of the bird - Parameters identification

The aim of this Chapter is to identify the parameters of the bird of interest. Although the parametric model is already elaborated, there is now a need for finding approximations of the dimensions of the sub bodies. The dimensions of interest are the Humerus length (HumL), the Ulna length (UlnL) and CarpoMetaCarpus length (CMCL). Moreover, in order to complete the parameters of the aerodynamic model, there is also a need to find estimations of the wing's characteristics i.e. wingspan (WS), wing area (WA) and aspect ratio (AR).

The main principle of this Chapter is to extrapolate the dimensions of the model from available data sets of birds. Note that the desired dimensions could be directly measured if the bird was at hand. However it is not the case. Therefore the following development should allow anyone to reproduce a similar model with their bird of interest. This approach should already provide a good estimation by only using this same data set. As a reminder, the bird of interest is the Northern Bald Ibis (Geronticus Eremita).

The available data set has been gathered by ourselves and is composed of four different sources. On one hand, there is the data set of Pennycuick [13] for the wings characteristics (WS, WA, AR). On the other hand, the bones dimensions are taken from Field [6], Simons [16] and Wang [20].

For the bones, Field, Simons and Wang give dimensions of Humerus length and diameter, Humerus, Ulna and CMC lengths and diameters and Humerus, Ulna, CMC and Primary feathers lengths (Fprim). The masses are taken from Dunning [5] for the data sets of Simons and Wang.

Even though their data sets are composed of birds of all sorts, it is only the birds from the ciconiiformes and pelecaniformes that will be used . The assumption made here is that the closer are those birds to the Geronticus Eremita, the closer the characteristics will be.

The followed development is inspired from Pennycuick, who has also from its own measurements searched for trends in birds dimensions. He only focused on the characteristics of the wings, i.e. wing span, wing area and aspect ratio. The common data of reference that he is using to establish the link between birds is the mass. It will be proceeded in the same way in the current approach. The reason is that the mass is the easiest data to obtain for any bird.

To summarize, the wing characteristics will be extrapolated first, and then the same development will be extended to the bones lengths and diameters.

To have an accurate model, the simulator need to have the values of masses, inertia, centers of masses, lengths of limbs and gravity. The data set of 220 bird species of Pennycuick [13], available at http://books.elsevier.com/companions/9780123742995, has made it possible.

As Pennycuick explains it, it is possible to extrapolate most of the missing data.

We are making here the assumption that birds of the same family will allow even more precise extrapolations the dimensions. Explicitly, this means that there are different species of ibises or

cousins that are proportionally similar to the bald ibis, even tough they have to be scaled up or down. They are different size versions of the bird with similar proportions.

1 Aerodynamic parameters - WS WA AR

Pennycuick while studying relations in bird scaling, made a few observations. First, it could be assumed that birds are following a simple isometric scaling. It means that for a given bird of mass X, if all its lengths were to be doubled, the mass of the new bird would be $8 * X$. It makes the assumption of constant density.

The isometric relationships are the following :

1. Length $\propto\ Mass^{\frac{1}{3}}$
2. Area $\propto\ Mass^{\frac{2}{3}}$
3. Volume $\propto\ Mass$

However, in reality, it is observed that the tendencies are allometric in opposition to isometric. The principle is to plot the wing span (length), wing area (area) and aspect ratio (no unit) against mass in double-logarithmic graphs and observe first, if there is a linear trend and second, if the slope is close to the isometric slope.

To summarize, we are using data from the following species :

Two other ibises, (Plegadis Chihi and Eudocimus Albus) and four pelicans cousins (Pelecanus erythrorhynchos, Pelecanus rufescens, Pelecanus onocrotalus, Pelecanus occidentalis) and one Ardeidae (Bubulcus Ibis). Note that other Ardeidae and ciconiiformes from the data set of Pennycuick could be taken.

These are all from the order of the Pelecaniformes, explicitly similar to pelican. Other cousins with the same type of flight are from the order of the Ardeidae and Ciconiidae . Storks, cranes and herons are part of it.

In order to find the aspect ratio, wing area and wing loading, the data set of Pennycuick will once again be used, with the same extrapolation.

The first value to fixed, which is the beginning of the development, is the mass. According to Dunning [5], the mean mass of a Geronticus Eremita is $m = 1.2\ [kg]$. This value will be kept identical for the whole paper. The plots of relationships are shown at Figures 4.1, 4.2 and 4.3. Three different lines are plotted : The isometric (Green), the one Pennycuick found with the extended data set of 220 birds (Blue) and the best fit for the current chosen subset (Red). In all cases, the best fit is the value kept.

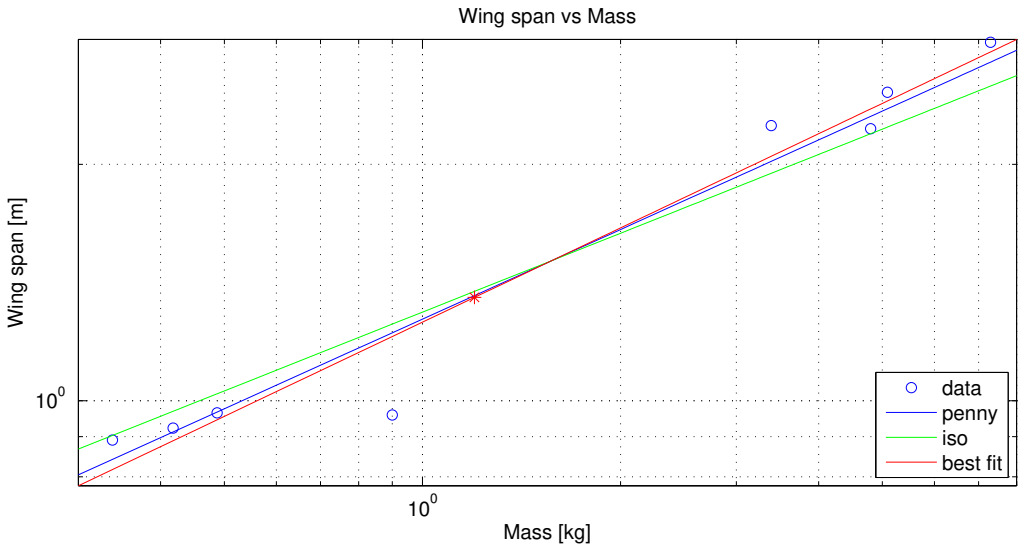

Figure 4.1 – Wing span extrapolation with the dataset of Pennucuick [13]. The "star dot" is the chosen value. Birds taxa used : Bubulcus ibis, Plegadis chihi (2), Eudocimus albus, Pelecanus erythrorhynchos, Pelecanus rufescens, Pelecanus onocrotalus, Pelecanus occidentalis.

The relationship between wing span and mass is given by the equation $WS = e^{0.2302} Mass^{0.3985}$. For a mass of 1.2 $[kg]$, we have $WS = 1.354$ $[m]$.

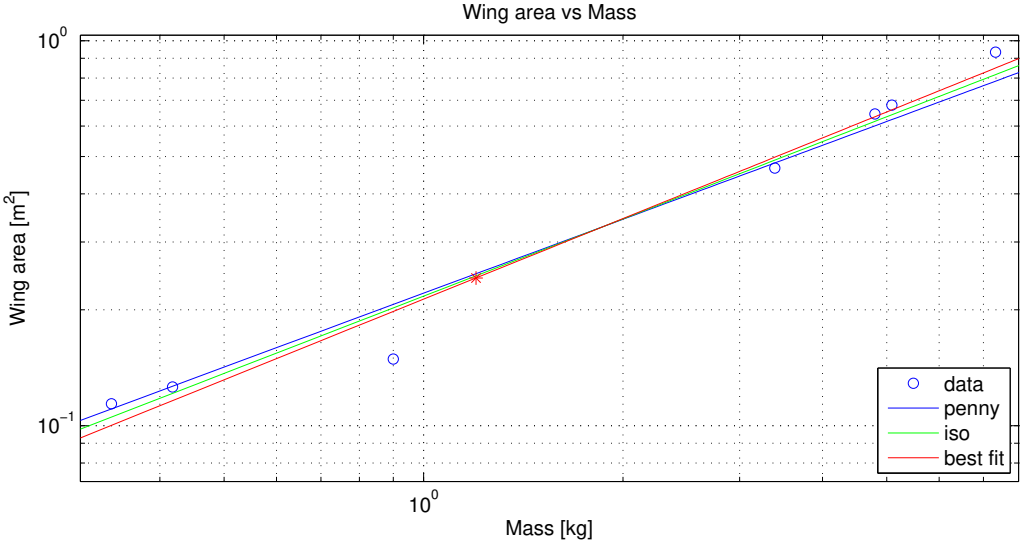

Figure 4.2 – Wing area extrapolation with the dataset of Pennucuick [13]. The "star dot" is the chosen value. Birds taxa used : Bubulcus Ibis, Eudocimus albus, Plegadis chihi, Pelecanus erythrorhynchos, Pelecanus rufescens, Pelecanus onocrotalus, Pelecanus occidentalis.

The relationship between wing area and mass is given by the equation $WA = e^{-1.5459} Mass^{0.6956}$. For a mass of 1.2 $[kg]$, we have $WA = 0.242$ $[m^2]$.

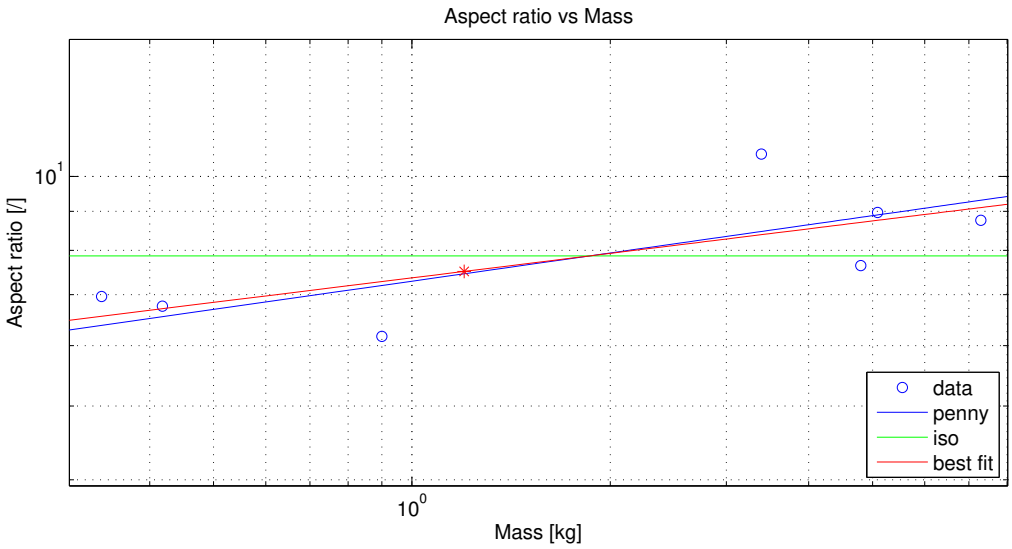

Figure 4.3 – Aspect ratio extrapolation with the dataset of Pennucuick [13]. The "star dot" is the chosen value. Birds taxa used : Bubulcus Ibis, Eudocimus albus, Plegadis chihi, Pelecanus erythrorhynchos, Pelecanus rufescens, Pelecanus onocrotalus, Pelecanus occidentalis.

The relationship between aspect ratio and mass is given by the equation $AR = e^{1.9964} Mass^{0.1068}$. For a mass of 1.2 $[kg]$, we have $AR = 7.507$ $[/]$.

It can be seen that for a range of masses from 300 $[g]$ to 7.3 $[kg]$, the trend is quite linear. It can be concluded that the Geronticus Eremita of 1.2 $[kg]$ should follow the same trend.

2 Structural parameters - Bones and feathers

Now, the same logic is applied to the data set of bones lengths. The results are plotted on Figures 4.4, 4.5, 4.6 and 4.7.

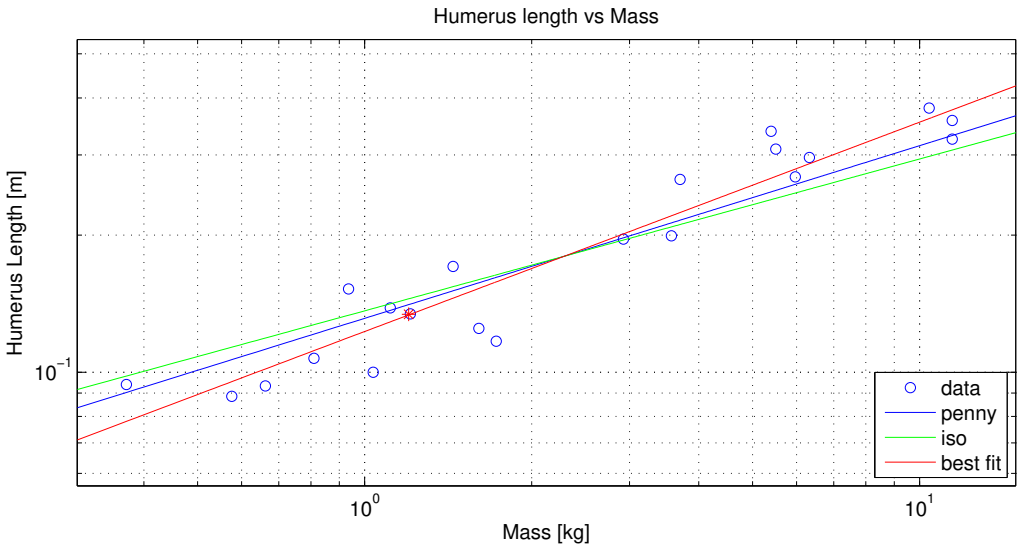

Figure 4.4 – Humerus length extrapolation with the dataset of Simons [16], Field [6] and Wang [20]. The "star dot" is the chosen value. Birds taxa used : Simons - Pelecanus erythrorhynchos, Pelecanus conspicillatus, Pelecanus crispus, Pelecanus occidentalis, Pelecanus onocrotalus, Pelecanus philippensis, Pelecanus rufescens; Field - Mesembrinibis cayennensis, Eudocimus albus, Theristicus caudatus, Threskiornis molucca; Wang : Nycticorax nycticorax, Ardea purpurea, Egretta alba, Ardea cinerea, Bubulcus ibis, Plegadis falcinellus, Botaurus stellaris, Ciconia nigra, Pelecanus onocrotalus, Ciconia ciconia.

The relationship between humerus length and mass is given by the equation $HumL = e^{-2.0966} Mass^{0.4595}$. For a mass of 1.2 $[kg]$, we have $HumL = 0.134$ $[m]$.

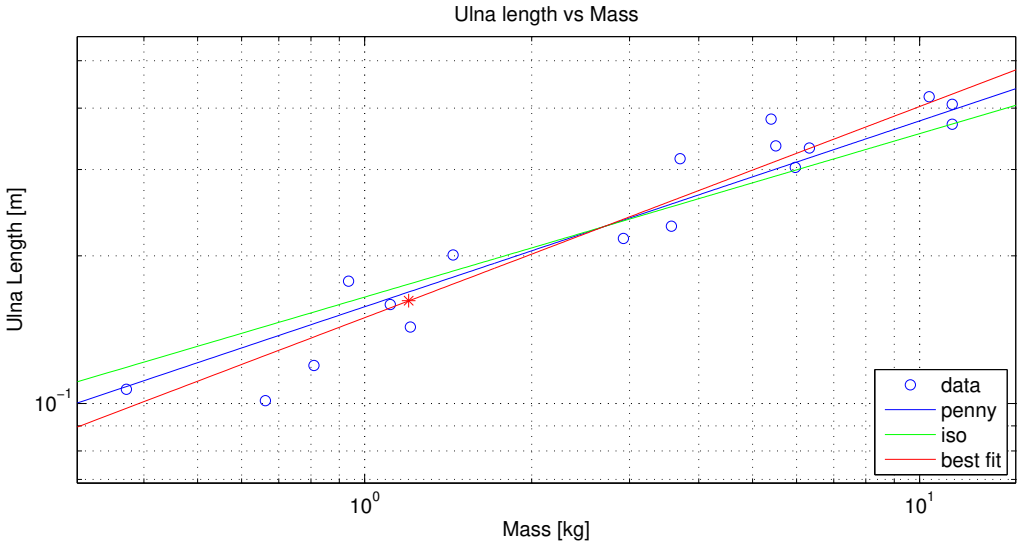

Figure 4.5 – Ulna length extrapolation with the dataset of Simons [16] and Wang [20]. The "star dot" is the chosen value.

The relationship between ulna length and mass is given by the equation $UlnL = e^{-1.8998} Mass^{0.4306}$. For a mass of 1.2 $[kg]$, we have $UlnL = 0.162$ $[m]$.

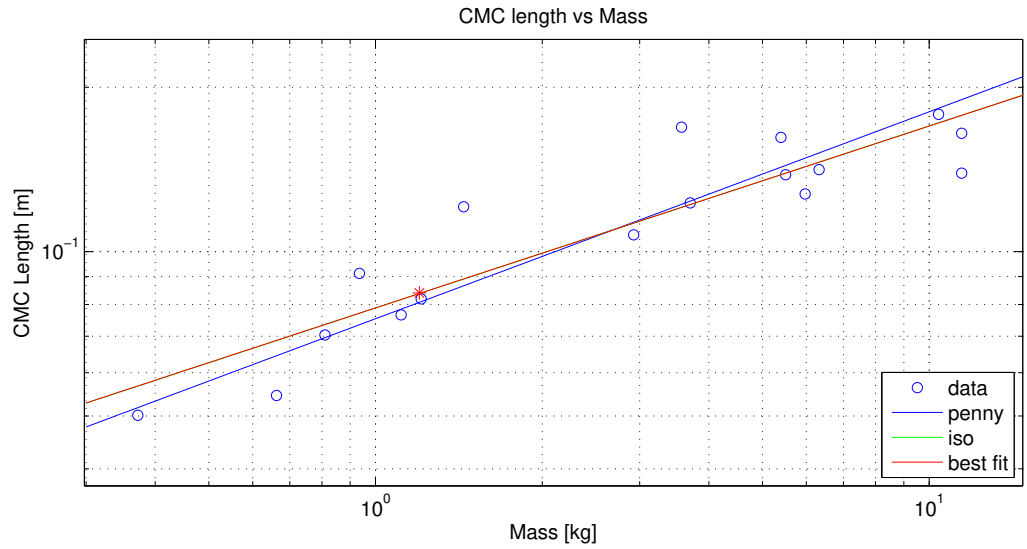

Figure 4.6 – Carpometacarpus length extrapolation with the dataset of Simons [16] and Wang [20]. The "star dot" is the chosen value.

The relationship between carpometacarpus length and mass is given by the equation $CMCL = e^{-2.54} Mass^{0.333}$. For a mass of 1.2 $[kg]$, we have $CMCL = 0.084$ $[m]$.

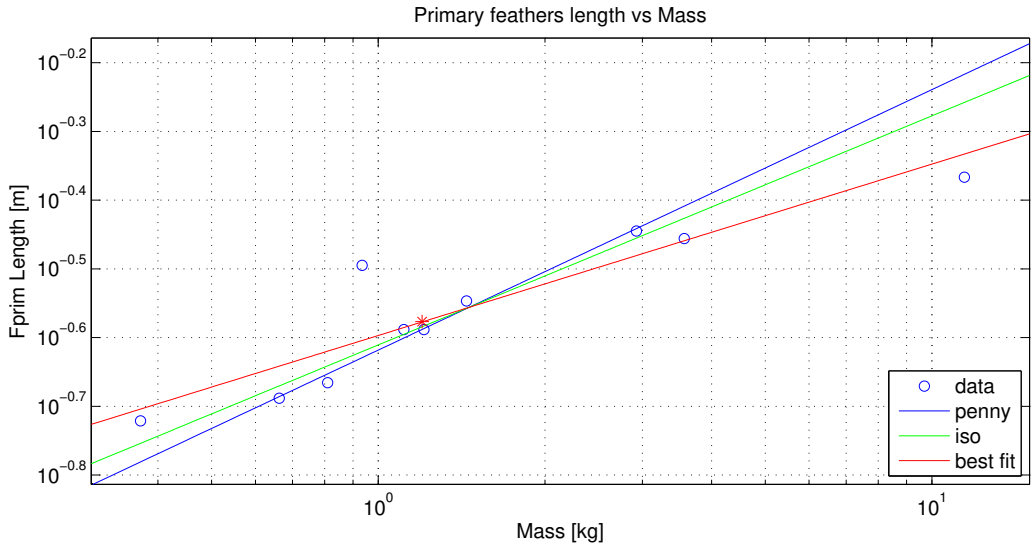

Figure 4.7 – Primary feather length extrapolation with the dataset of Wang [20]. The "star dot" is the chosen value.

The relationship between primary feather length and mass is given by the equation $FprimL = e^{-1.3744} Mass^{0.2494}$. For a mass of 1.2 $[kg]$, we have $FprimL = 0.265$ $[m]$.

Concerning the lengths, only one value remains to be found : the distance between the two shoulder fixations, also called inter-coracoid space.

As no other data was found for this value, the only solution is to measure it on pictures of skeletons of birds. In order to do this, measure is taken on a pigeon skeleton. Because of the lack of data, a simple isometric relationship is assumed, keeping the proportions identical. The result is that the Inter-Coracoid Space is $ICS = 0.092$ $[m]$

Thanks to [?], we can also double check the result (+ pictures from bald ibis?) to be sure it stays within the standard deviation.

Chapter 5

Kinematic analysis of the flight

The purpose of this Chapter is to identify the kinematics of flight of the Geronticus Eremita. Given the small amount of data available, the goal will be to have approached kinematics that would be good enough for flying. In order to find a more effective way of flying, other methods could be later used such as optimization. Alternatively, measuring more precise data could be useful. First of all, all the parameters for one beat need to be identified. Then the fly of a Geronticus will be analyzed first, qualitatively and afterwards, quantitatively. The data used for the analysis is a video recording of a Geronticus Eremita.

After the analysis, the resultant flight will be compared to the real flight video and to data of flight of other birds i.e. magpie and pigeon.

1 Types of flight in nature

This section will focus on the study of the bird flight. Now that a first mechanical model has been depicted, the goal is to find the correct kinematics thereof, respecting the real movement of the Bald Ibis.

They are four main types of flight. Each bird is usually using one type or in between two [21].

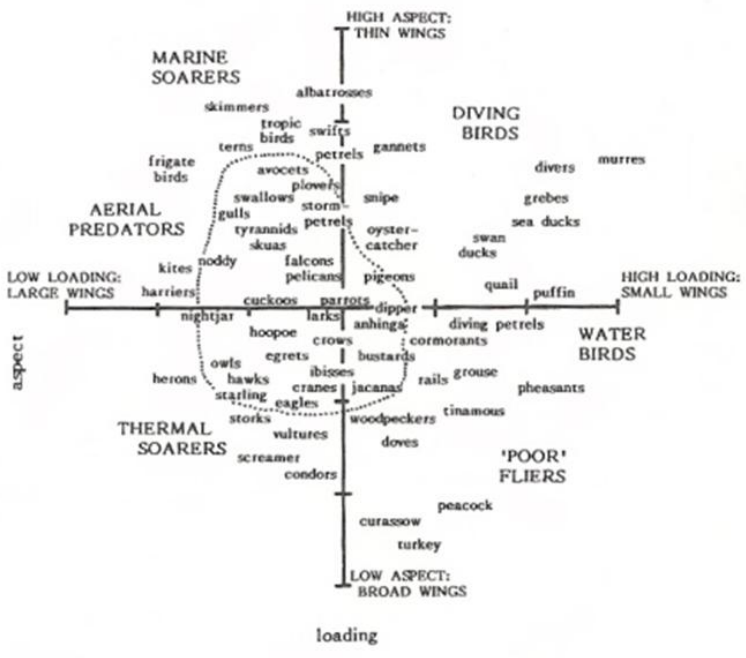

Figure 5.1 – Wing loading versus Aspect ratio. The ibisses appear on the schematic to be average flyers. They are quite close to egrets and cranes and less from herons and pelicans. (Figure taken from http://people.eku.edu/ritchisong/554notes2.html)

As it can be seen on Figure 5.1, the two main parameters that define the type of flight are the Wing loading and the Aspect ratio.

The ibises have a tendency to be more of the thermal soarers. Moreover, they are defined as FS : "Flapping - Soaring" flyer.

2 Parameters of the flapping flight

Note here that in our case we are only interested for now in the analysis of a steady speed and constant height flight. The bird is analyzed in a situation of flapping flight. As it was already mentioned on Figure 2.3, the kinematics of a wing for a bird can be seen as a composition of three movements : wing folding, wing twisting and wrist flexing. Added to those, there are also the general orientation of the wing and the beating of the wing. As a reminder from Chapter 2, there are 7 DOF for each wing. In this chapter, they are called : $q_{beat}(t)$, $q_{sh-ori}(t)$, $q_{sh-fold}(t)$ for the shoulder, $q_{elb-fold}(t)$, $q_{twist}(t)$ for the elbow and $q_{wst-fold}(t)$, $q_{Rwst}(t)$ for the wrist. They are supposed to be functions of time and must be found. As the movement is assumed to be symmetric, they will be the same for left and right wing. $q_{sh-fold}(t)$, $q_{elb-fold}(t)$ and $q_{wst-fold}(t)$ are responsible for the folding movement, $q_{twist}(t)$ for the twisting, $q_{Rwst}(t)$ for the wrist flexing, $q_{beat}(t)$ for the wing beat and $q_{sh-ori}(t)$ for the shoulder orientation.

A first assumption is that all the functions are periodic of the same or multiple of the frequency of wing beat.

As the whole movement is supposed to be periodic, sinusoidal functions have been chosen to fit to the recorded data. The general formulation used is shown on Equation 5.1. Frequency is supposed to be the same for all DOF even tough it is a parameter that will be found later on. For each DOF, it means that there are 3 unknowns that still need an equation to solve the system.

$$q_i(t) = A_i \ \sin\left(2\pi f t + \phi_i\right) + A_{0i} \tag{5.1}$$

Reminder of the assumptions made :

1. The beating is a periodic motion, even if it can be modulated in function of the environment : it means that wing folding, wrist twisting and flexing can be characterized by periodic function that are of same frequency or multiples.

2. The movement of both wings is supposed to be perfectly symmetric.

2.1 Qualitative analysis

The available data comes from a video recording. It will allow to analyze the front view kinematics of the bird. Each picture has been taken at each time frame. In the recording, video had 24 frames per second so that these 24 pictures cover one second (See Figure 5.2). Although the measure are partially imprecise, it will already give a good insight of the flight.

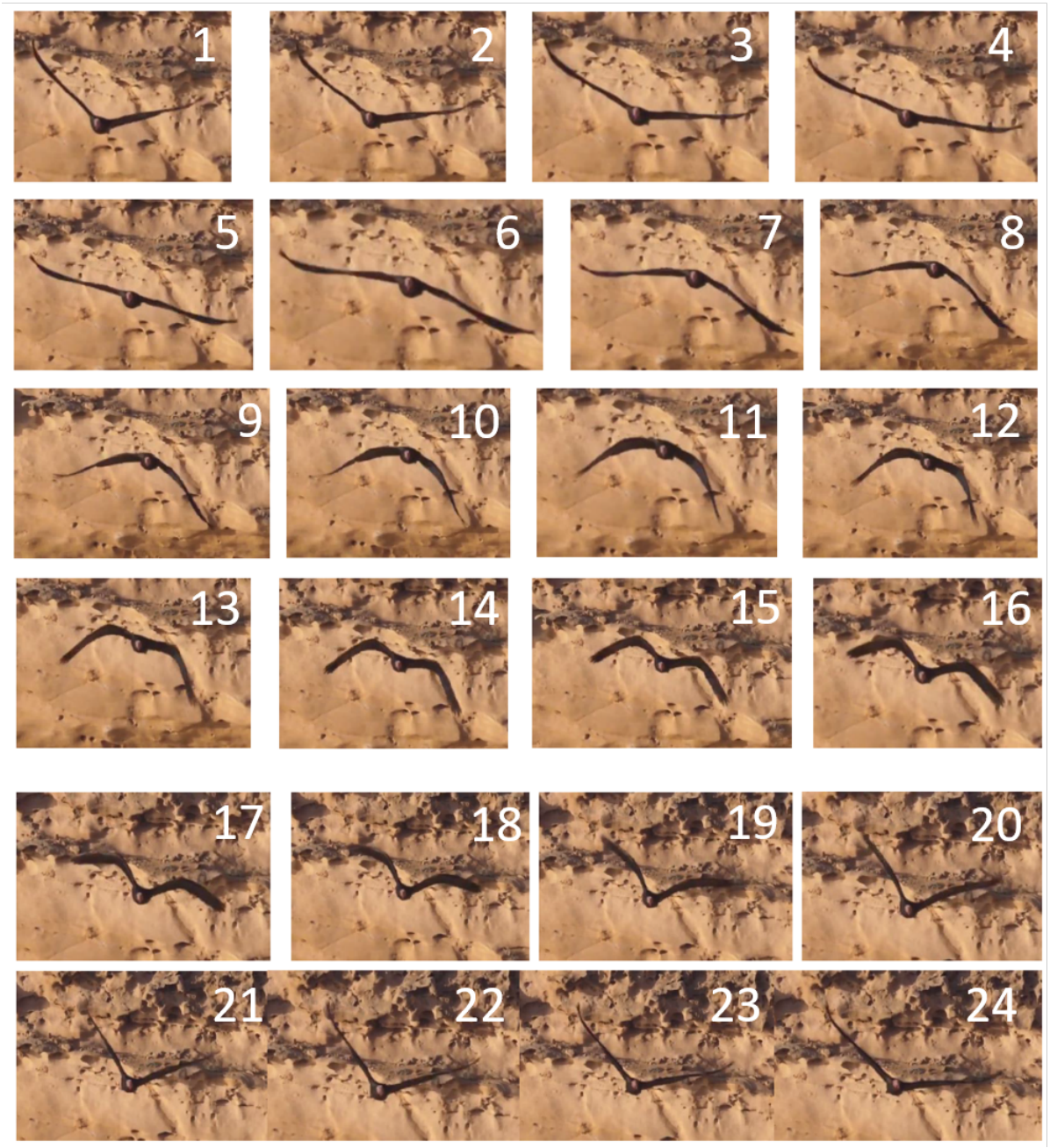

Figure 5.2 – Frontal view - Kinematic data of the Geronticus Eremita. The video recording is a slow motion of 24 frames/second. The set of 24 pictures represent 1 second and all pictures are equally spaced in time. The 24 pictures cover a complete cycle of one beating. The frequency and speed are unknown. (Based on video recording taken from https://www.youtube.com/watch?v=QGx4olNnbTQ)

A first observation of the pictures shows that the extrema of the beating and wrist flexing are quite obvious to measure as they have a large amplitude. It will allow the measures of the amplitudes and offsets of q_{beat} and q_{Rwrist}. The definition for the measurement of these two angles is shown on Figure 5.3.

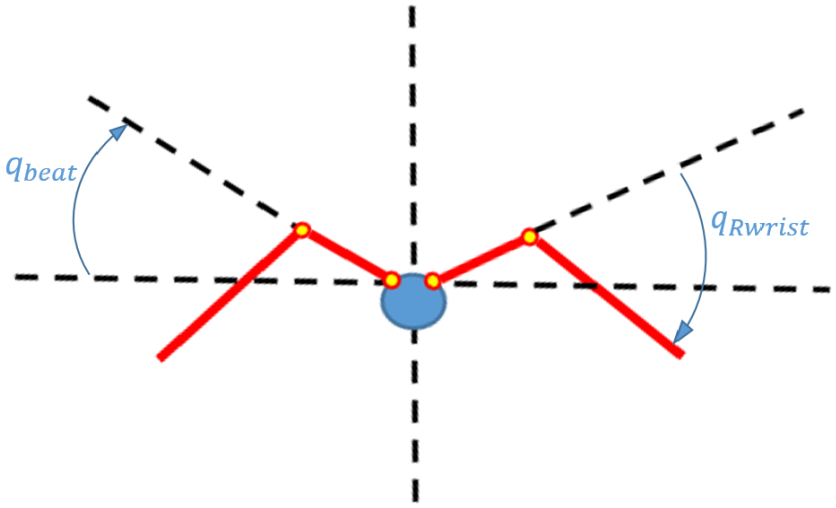

Figure 5.3 – Frontal view - Definition of the measured angles. q_{beat} is measured from the plane perpendicular to the plane of symmetry of the bird. They are respectively the horizontal and vertical dashed lines. q_{Rwrist} is measured from the line parallel to the segment [shoulder - Wrist] of the wing.

An interesting observation of the pictures, concerning the wrist flexion (q_{Rwrist}), is that the wrist seems to break at the beginning of the upstroke. From an aerodynamic point of view, it is perfectly normal because it minimizes the wing area which is proportional to lift and drag forces. It is the way that the bird produces a difference of lift between upstroke and downstroke in order to compensate for its weight. It also seems to more or less recover and realign with the rest of the arm at the beginning of the upstroke. However, during the whole downstroke, the wrist flexing is kept at zero.

It can also already be observed that $q_{twist}(t)$ and $q_{sh-ori}(t)$ seem quite small in amplitude compared to q_{beat} and q_{Rwrist}, at least for this straight flight. q_{beat} and q_{Rwrist} are already independent from the folding functions. If $q_{twist}(t)$ and $q_{sh-ori}(t)$ can be assumed small, they would have negligible impact on the measure of q_{beat} and q_{Rwrist}. Concerning the folding functions $q_{sh-fold}(t)$, $q_{elb-fold}(t)$ and $q_{wst-fold}(t)$, the front data kinematics give few insight for possible interpretation.

2.2 Quantitative analysis

Now that general qualitative observations have been made, the goal is to find numeric values to all the parameters of the 7 functions.

Beat q_{beat} and wrist flexing q_{Rwrist}

First, q_{beat} and q_{Rwrist} can be found. As we assume that the orientation ($q_{sh-ori}(t)$) and twisting ($q_{twist}(t)$) have negligible influence on them, the raw data from measures can be used by taking the extremas of amplitude of q_{beat} and q_{Rwrist}. The frame number is also important as it is the time reference. The result : q_{beat} is going from 53° (Frames 19 20) to −18° (Frame 9). It gives the amplitude $A_{beat} = 35°$ and the offset $A_{0-beat} = 17°$. q_{Rwrist} is going from approximately 0° (Frames 1 2 3 4 5 6 7 21 22 23 24) to 72° (Frames 14 15 16). The data does not seem to correspond to a simple sine function. By plotting it against time, the observations and approximations are confirmed (See Figure 5.4).

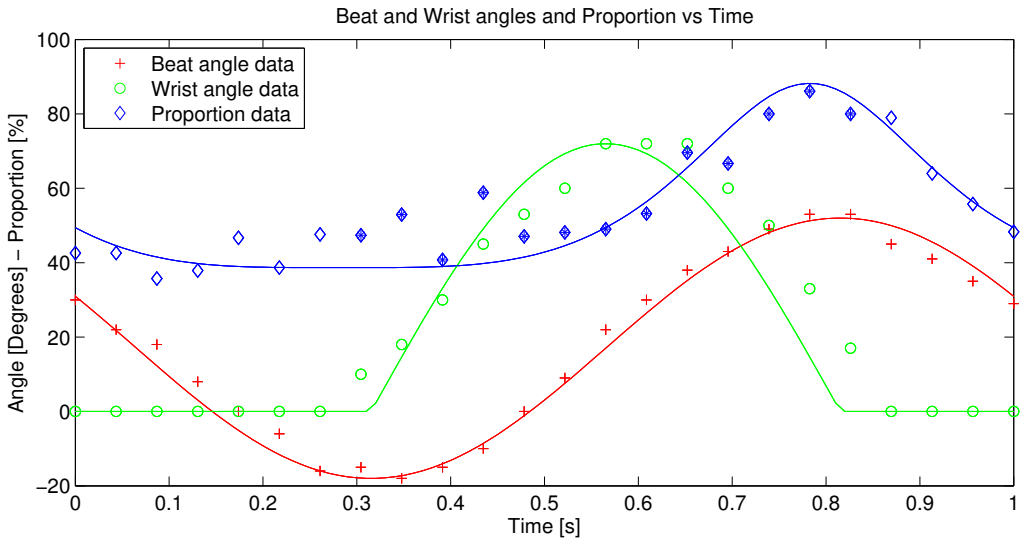

Figure 5.4 – Plot of the data (q_{beat}, q_{Rwrist} and the proportion) measured from the video recording and their approximated function chosen by ourselves. The beat and wrist angles are a close approximation, but the proportion between the shoulder-wrist segment and the outer part of the wing is still partially imprecise. Proportion is the value $p = \frac{a}{d(t)}$ on Figure 5.9.

As shown on Figure 5.4, the beat function is close to the behaviour of a pure sine function. Concerning the wrist flexing, a better choice is a half sine function. Half of the cycle, it is forced to zero and the other half behave like a simple sine. For convenience, the function is still assumed to have the same frequency as the other functions. The beginning and ending of q_{Rwrist} are supposed to situate on the extremas of the beating in order to minimize the lift during the upstroke. Therefore, the final choice is to take the maximum of q_{Rwrist} for the amplitude of the sine, even though it is not reaching its maximum at the same time as in the data. We have $A_{Rwrist} = 72°$ and $A_{0-Rwrist} = 0°$.

Wing folding - $q_{sh-fold}$ $q_{elb-fold}$ $q_{wst-fold}$

Concerning the folding functions, the data set of the front kinematics is not sufficient. However, observations from the literature could give more insight. The following observations are based on the work of Tobalske [17] and his measurements of wing kinematics for pigeons and magpie. Taken from his work, Figures 5.7 and 5.6 show dorsal view of the wingtip and wrist kinematics for those birds.

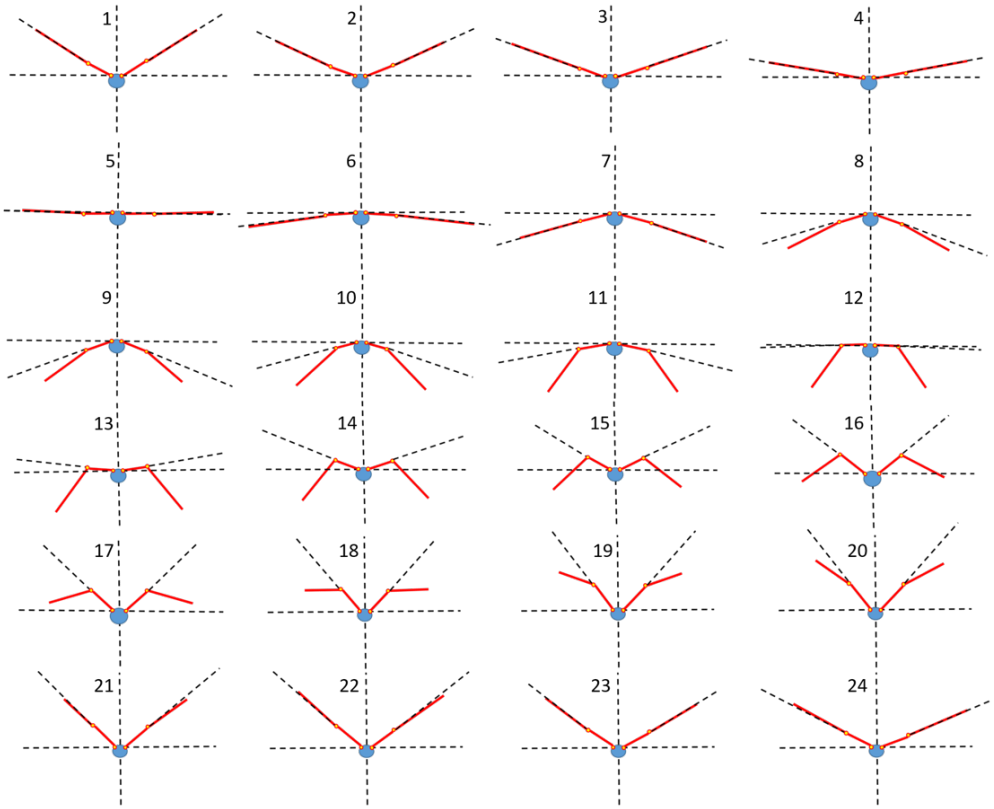

Figure 5.5 – Frontal view - Kinematic data of the Geronticus Eremita cleaned and represent on an horizontal frame. The measures are taken from that data set for the kinematics.

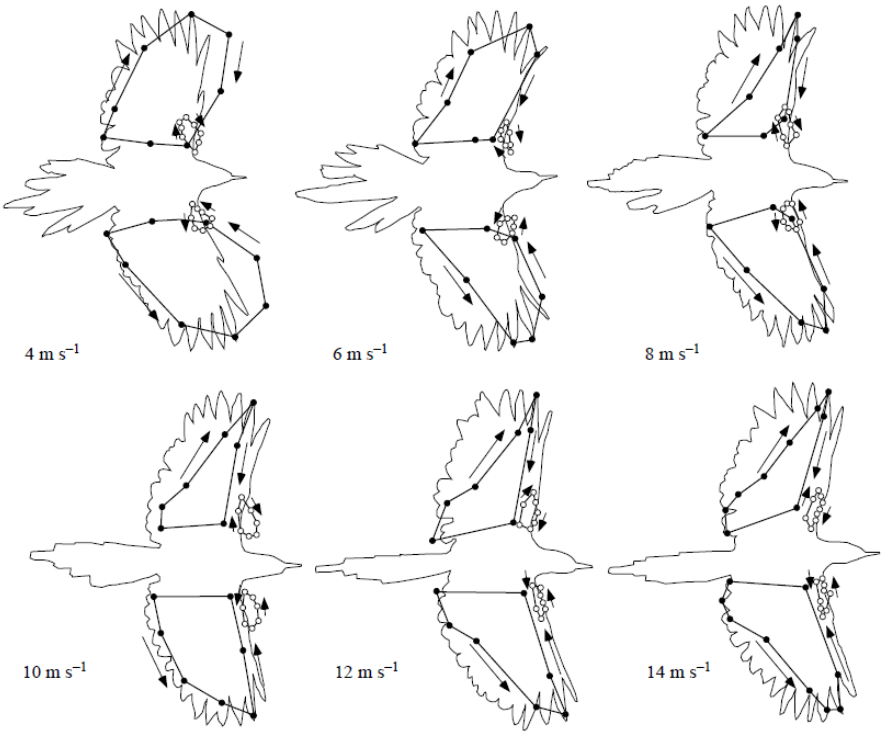

Figure 5.6 – Kinematics data of the flight of the magpie over speed from 4 to 14 $[\frac{m}{s}]$ - Dorsal view (Figure taken from Tobalske [17])

From these Figures, one can see that the wrist position has a really small amplitude of movement compare to the wing tip. Moreover, part of the amplitude visible on dorsal view is only due to movement of beating and not to the expansion of the wrist. It is then decided to make the assumption that the folding of the elbow and shoulder are constant for a flight in steady state. Therefore, the shoulder and elbow expansions, $q_{sh-fold}$ $q_{elb-fold}$ are approximated to two constants. The constants still need to be found. Note that it is not the case of $q_{wst-fold}$, as the last function for folding the wing is responsible for the movement of high amplitude of the wing tip. It seems, given the high amplitude of the wing tip movement, that this function has a main impact.

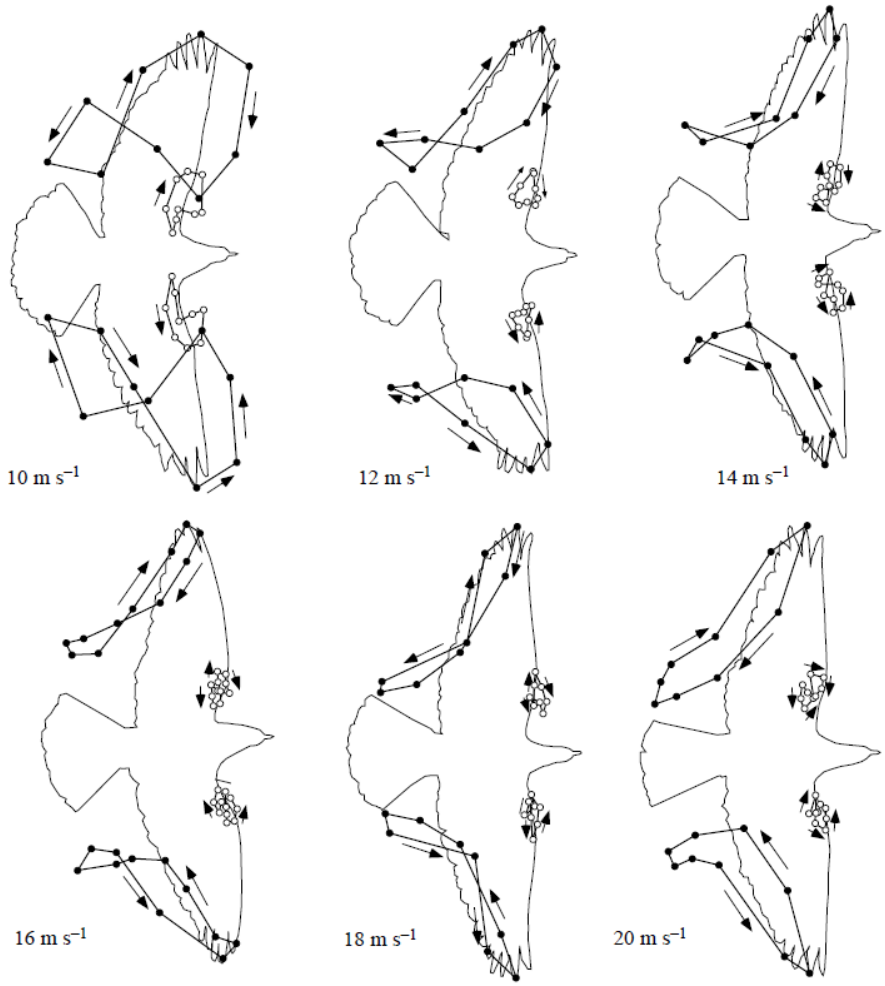

Figure 5.7 – Kinematics data of the flight of the pigeon over speed from 10 to 20 $[\frac{m}{s}]$ - Dorsal view (Figure taken from Tobalske [17])

In order to find the constant positions of the shoulder and elbow folding functions ($q_{sh-fold}$, $q_{elb-fold}$), the following development has been chosen : The angle of the shoulder and elbow can be found following this reasoning. The wrist joint is assumed to stay in the same plane during the whole beating. It means that in lateral view, the wrist would only draw a line for its movement. On the lateral views of the pigeons and magpies, it can be seen that the wrist lines are also almost drawing lines and not ellipsoids. (See Figures 5.18 and 5.17.) From this assumption, and by taking the wing in the situation of maximum span, it is possible to link the wingspan previously found and all the lengths of the bones also previously found. The Figure 5.8 shows more graphically the geometric assumption. The lengths b and c are known because they are the bones lengths : $b = 162$ $[mm]$ and $c = 134$ $[mm]$.

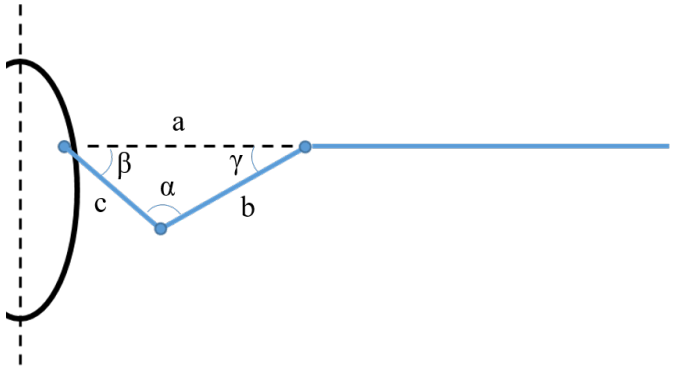

Figure 5.8 – Law of cosine on the positioning of the wrists along the axis of alignment of both shoulders - Dorsal view

Knowing that, both angles can be found by using the equation of Generalized Cosine. The purpose here is to find the α, β and γ angles which is equivalent as finding the constants $q_{sh-fold}$ and $q_{elb-fold}$.

$$b^2 = a^2 + c^2 - 2ac\cos\beta \tag{5.2}$$

In order to find the three angles of interest, there is only the length a left to find. Here is the chosen method : The lengths of all bones and primary feathers are known as well as the wing span and inter-coracoid space (Reminder : the space between the two shoulder joints). The purpose is here to make the wing span and these bones dimensions match. As the bones aligned on a straight line give a larger wing span, the elbow and shoulder have to fold partially. This will allow the computing of the length a. The inter-coracoid length is $ICS = 92$ $[mm]$, wing span is $WS = 1354$ $[mm]$. The most extreme primary feather is still assumed to be aligned with the phalanx and carpometacarpus so that the sum of them is $CMCL + FprimL = 84 + 265 = 349$ $[mm]$. The final result for a is $a = \frac{WS}{2} - \frac{ICS}{2} - (CMCL + FprimL) = 282$ $[mm]$.

The final result for β is :

$$\beta = \arccos\left(\frac{a^2 + c^2 - b^2}{2ac}\right) = 19.5 \approx 20^\circ \tag{5.3}$$

Now, there is still the expansion of the wrist to be found, i.e. $q_{wst-fold}$. From the data of other birds (Figures 5.18 and 5.17), and from the video recording of the Geronticus Eremita, it seems that the wingtip on lateral view, is close to a kind of ellipsoid. As the beating, i.e. the movement on z-axis on the lateral view, is already a sinusoidal function, another sinusoidal function in the expansion of the wrist will result in a sinusoidal movement on the x-axis of lateral view and also in an ellipsoid. As there are no precise data available for $q_{wst-fold}$, the method used is the following.

The distance wrist shoulder is measured on all the pictures of the Geronticus Eremita and compared to the distance wrist wingtip. As the distance wrist shoulder is supposed to remain in the same plane at any time, all time frames can be compared to see the evolution of the wrist wingtip in frontal view. The measures are also displayed on Figure 5.4 as Proportion expressed in percentage. It is the value $p = \frac{a}{d}$ on Figure 5.9.

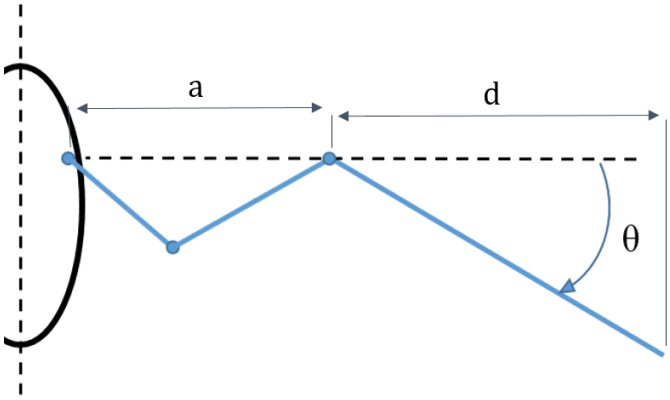

Figure 5.9 – Definition of the folding/extending of the wrist. The angle is measured from the dashed line, i.e. the alignment of the segment [shoulder - wirst] and the carpometacarpus. - Dorsal view

Finding the angle θ is equal to find the double of the amplitude of $q_{wst-fold}$ as it is a sine oscillating between 0 and θ. We first define the proportion at the extremas : $p_{max} = \frac{a}{d_{min}}$ and $p_{min} = \frac{a}{d_{max}}$. We can then say that $\cos\theta_{max} = \frac{d_{min}}{d_{max}} = \frac{p_{min}}{p_{max}}$. The final resulting equation is :

$$\theta_{max} = \arccos\left(\frac{p_{max}}{p_{min}}\right) \tag{5.4}$$

In our case, from the measures, we have $p_{max} = 0.8611$ $p_{min} = 0.3867$. The final result is $\theta_{max} = 63°$ and an amplitude $A_{wst-fold} = -32°$. Concerning all the phases ϕ_i of the time functions, the beat is considered to be the time reference so that it is zero in $t = 0$. From there, $\phi_{Rwrist} = pi/2$ to reach its maximum when the beating is in the middle of the oscillation. The phase of $q_{wst-fold}$ is $\phi_{wst-fold} = -2.94$ $[rad]$.

Wing orientation and twisting - q_{sh-ori} q_{twist}

About the wrist twisting and the general orientation of the shoulder, the analysis is simplified. The twist movement is not covering a wide range of angles and so that it can be approximated to zero for now (It could have more importance when it comes to fine tuning of the flight). It only leaves the orientation as final parameter.

Before the last parameter is finally fixed, the bird is already tested to see its ability to fly. The result is that the bird is already flying in open loop. However it is not yet naturally stabilizing at constant speed and height. Nevertheless, after a small tuning of the general orientation of the shoulder, still in open loop, the bird has found an equilibrium in steady state at constant speed and height. Note that this tuning consists only in finding the right constant angle for the general orientation.

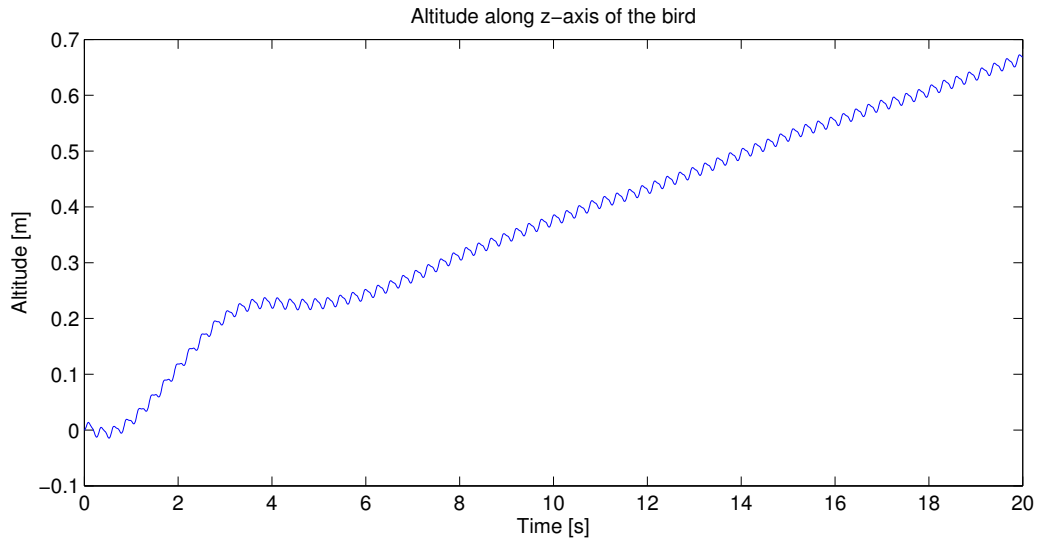

Figure 5.10 – Altitude of the bird along the z-axis. The simulation is obtain with wind speed of 12.7 $[\frac{m}{s}]$ with respect to the bird body which is close to its stabilizing speed. The orientation angle of the wing is $-3°$.

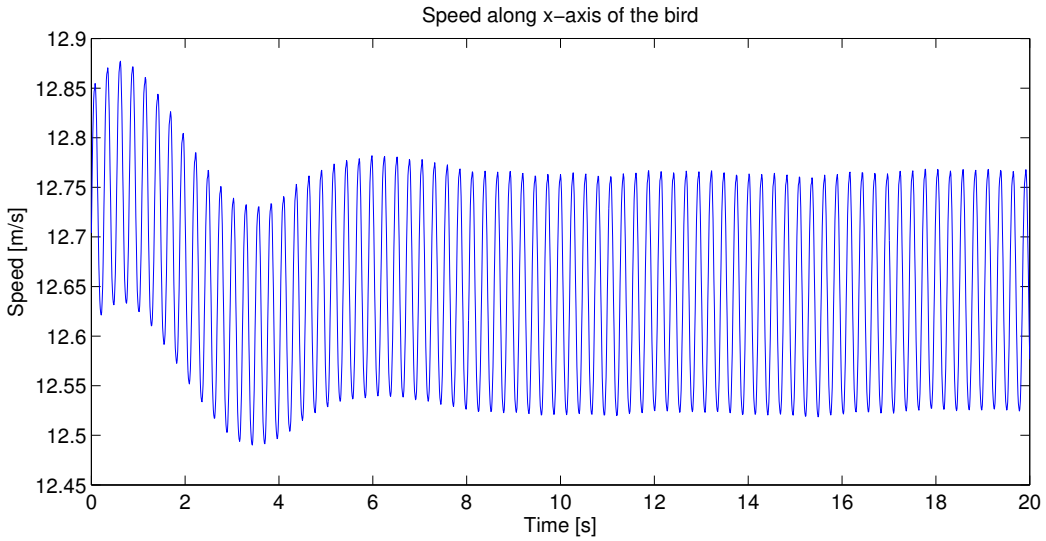

Figure 5.11 – Speed of the bird along the x-axis. The simulation is obtain with wind speed of 12.7 $[\frac{m}{s}]$ with respect to the bird body. 12.7 $[\frac{m}{s}]$ is the average stabilizing speed. The orientation angle of the wing is $-3°$.

Finding this equilibrium is equivalent to finding the right equilibrium between drag and lift forces. If the angle of attack increases, the bird is generating more lift while the drag is also increasing. This means that the bird is gaining in height but slowing down. By changing the orientation of the wing, one can change the equivalent angle of attack thereof. This result is perfectly logic. Moreover, it is convenient as it means that the bird is already stable in open loop and there is no need for now to do feedback to stabilize the system. Results are shown on Figures 5.12 and 5.13.

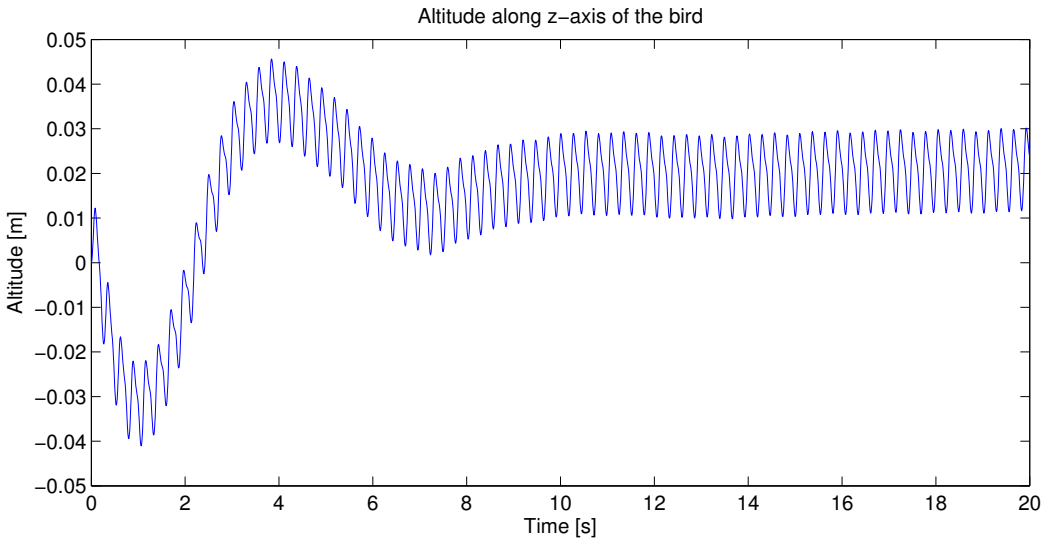

Figure 5.12 – Altitude of the bird along the z-axis. The simulation is obtain with wind speed of 12.7 $[\frac{m}{s}]$ with respect to the bird body which is close to its stabilizing speed. The bird takes about 10 second of transient dynamic before stabilizing. A slight drift is observable after stabilization. An oscillation of the altitude of about 2 $[cm]$ is observable, due to the beating. The orientation angle of the wing is $-2.378°$.

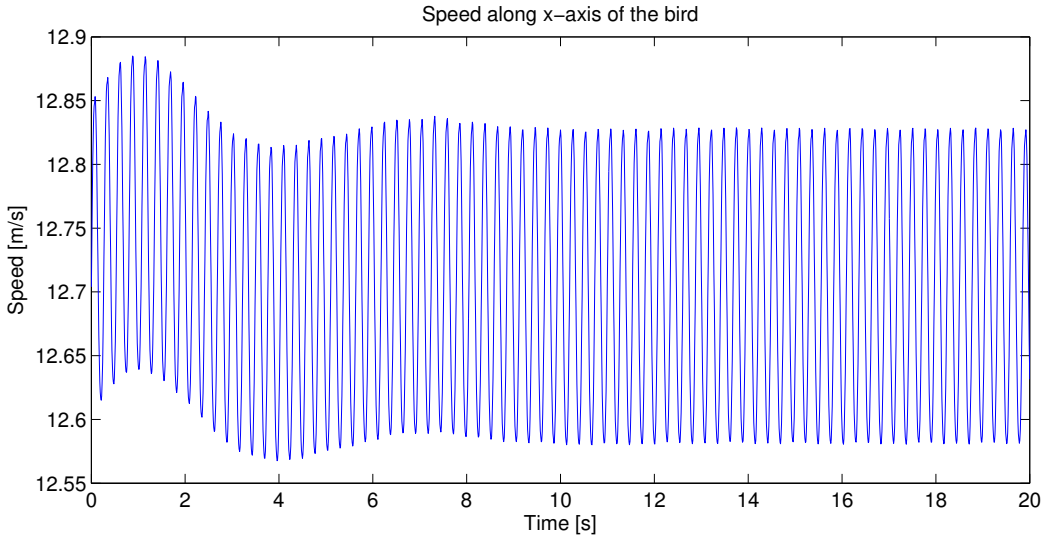

Figure 5.13 – Speed of the bird along the x-axis. The simulation is obtain with wind speed of 12.7 $[\frac{m}{s}]$ with respect to the bird body. 12.7 $[\frac{m}{s}]$ is the average stabilizing speed. The bird takes also about 10 second of transient dynamic before stabilizing. An oscillation of the speed of about 0.25 $[\frac{m}{s}]$ is observable, due to the beating. The orientation angle of the wing is $-2.378°$.

Finally, it is necessary to choose which speed and beat frequency the bird is supposed to fly. According to the work of Pennycuick [13], a good approximation for minimum power flight speed and beat frequency is based on Equation 5.5.

$$f = m^{\frac{3}{8}}\ g^{\frac{1}{2}}\ B^{-\frac{23}{24}}\ S^{-\frac{1}{3}}\ \rho^{-\frac{3}{8}} \tag{5.5}$$

$$f = 1.2^{\frac{3}{8}}\ 9.81^{\frac{1}{2}}\ 1.354^{-\frac{23}{24}}\ 0.2419^{-\frac{1}{3}}\ 1.225^{-\frac{3}{8}} = 3.73\ [Hz] \tag{5.6}$$

3 Comparison with existing flight data

This section is dedicated to a comparison of the results obtained from the multiple simplifications and the video recording as well as data from the pigeon and magpie. The Robotran results can be seen on Figure 5.14. These results can be compared to the front flight of the recording.

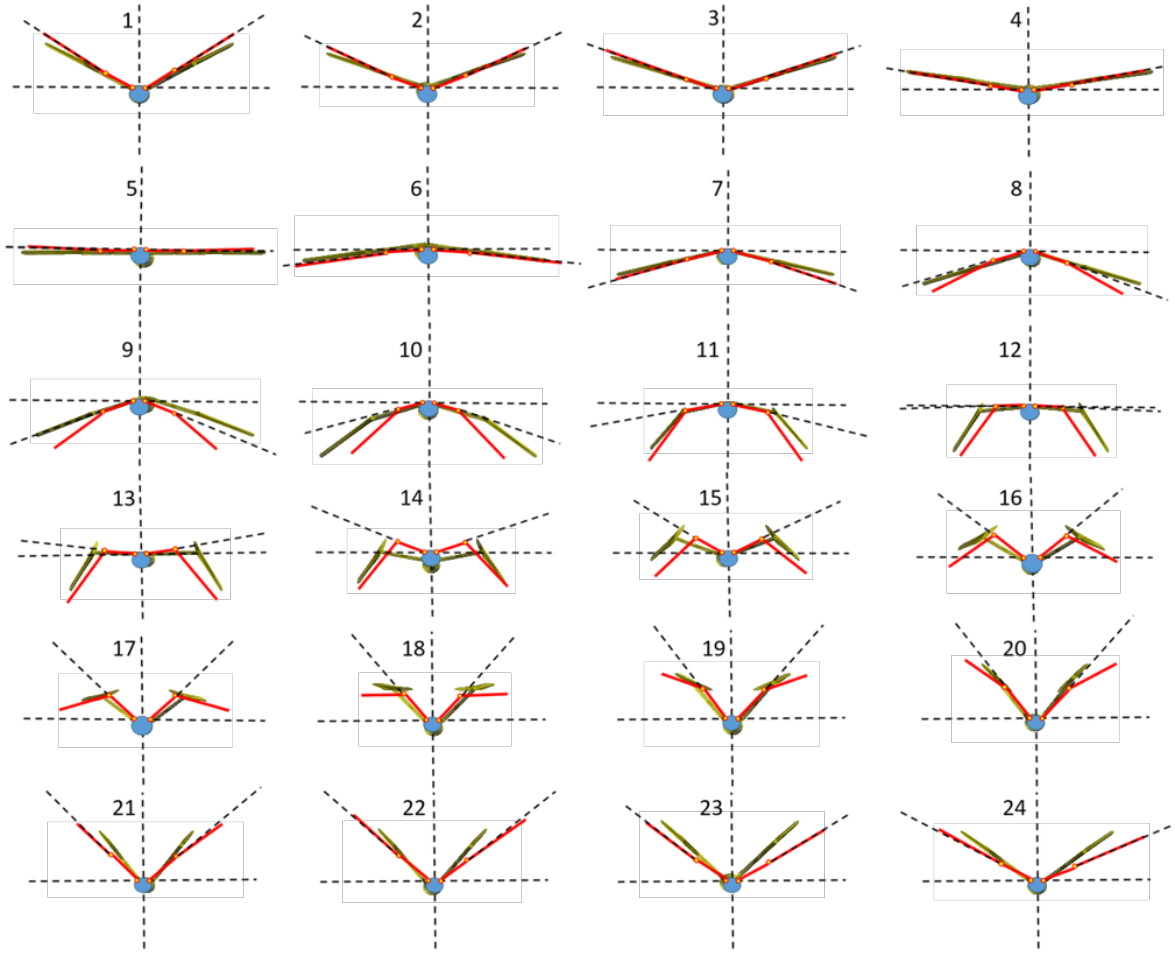

Figure 5.14 – Results of the simplified kinematics in Robotran compared to the measurements over a complete wingbeat cycle (Red : measures; Green : Robotran) - Frontal view

There is also dorsal and lateral views visible on Figure 5.15 and 5.16 that can be compared to the data of the magpie and pigeon of Figures 5.17, 5.6, 5.18 and 5.7.

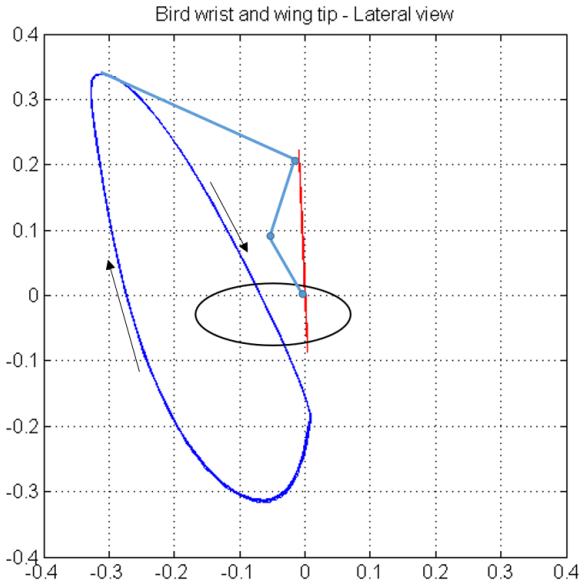

Figure 5.15 – Wingtip and wrist lateral view (Red : wrist; Blue : wing tip)

As expected, the lateral data also gives an ellipsoid-like form. However, the dorsal view seems quite different. This can be due to the simplifications. Nevertheless, one should keep in mind that as the two bird species are already quite different and the Geronticus being quite larger, it is also natural to obtain differences. Heavier birds, generally generate less movement of wings, as the mechanical power that would be required would be higher.

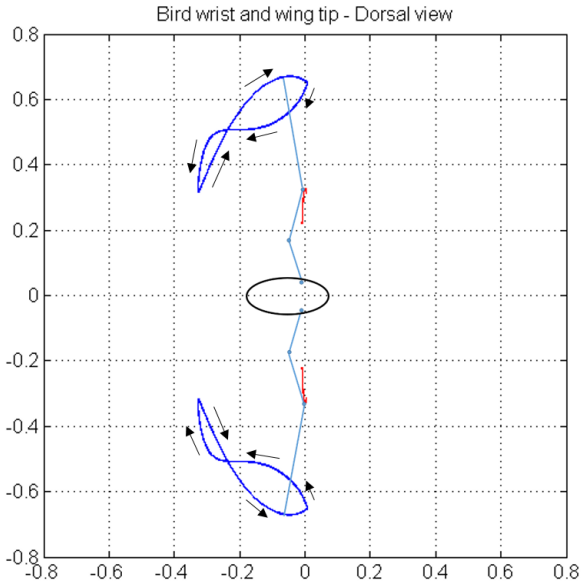

Figure 5.16 – Wingtip and wrist dorsal view (Red : wrist; Blue : wing tip)

The goal here will then to tune the right parameters of these different movements in order to achieve the natural movement of the bird.

However, there is no real data from Bald ibis or such large birds with similar type of wing loading and aspect ratio.

Nevertheless, it will already be a good benchmark to compare it to data from a pigeon, which has the flight the most similar to the ibis's one.

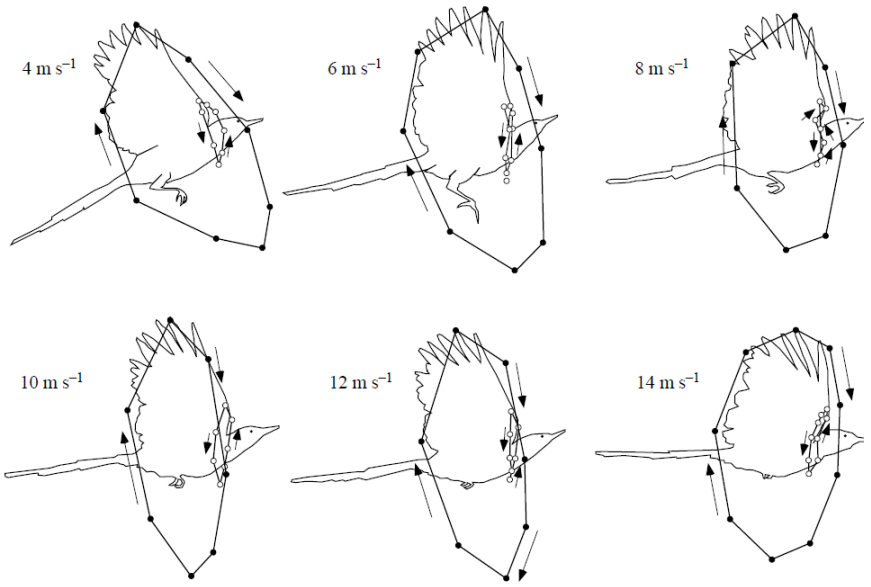

Figure 5.17 – Kinematics data of the flight of the magpie over speed from 4 to 14 $[\frac{m}{s}]$ - Lateral view (Figure taken from Tobalske [17])

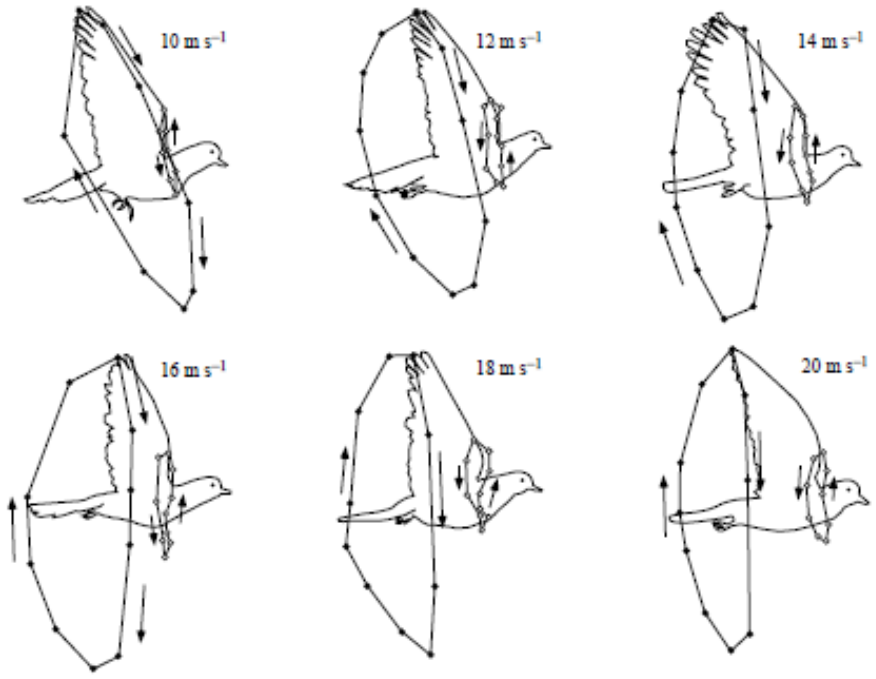

Figure 5.18 – Kinematics data of the flight of the pigeon over speed from 10 to 20 $[\frac{m}{s}]$ - Dorsal view (Figure taken from Tobalske [17])

Moreover, there are still videos of flying pelicans and ibises, which can help to visually check for a possible similarity.

The next goal is to plot the kinematics of the model and compare it with the available data.

Chapter 6

Actuation by muscles modelling

In the past chapters, the movement of the bird was constrained kinematically. However, the objective of this thesis is to add an actuation of the movement that is bio inspired. This step will allow later work to create a stimulation generator. The complete system will be as close to the real bird as possible. It is the purpose of this Chapter.

First of all, the model of muscle used, i.e. the Hill muscle-tendon model, will be more detailed. A particular focus will be dedicated to the inversion of the model. The reason is that the stimulation patterns applied to the muscles are unknown. Therefore, first, the joint torques will be extracted from Robotran for the desired motion. Second, by inverting the muscle model, one would obtain the activation patterns necessary. Finally, to validate the reasoning, these patterns should be re-applied to the Bird and muscles system and achieve the same motion. A special attention is devoted to solving the general problem of over-actuation for any composition of muscles.

Note that to make this work there are many missing parameters, especially concerning the muscles characteristics. How to obtain realistic values will also be further developed.

1 Selection of the muscles

The goal of the section is to find the right set of actuating muscles. There are about 50 different muscles responsible for the actuation of one wing. It is way too much to model and would make the model too heavy, hence to slow for simulations. The method here is to logically cover the muscles and see which ones are useful for the main movements in our kinematics. Here are the main movements necessary :

1. Shoulder joints :
    - Elevate/Depress the wing [Beating]
    - Pronate/Supinate the wing [Orientation]
    - Abduct/Adduct the wing [Expansion]
2. Elbow joints :
    - Flex/Extend the elbow [Expansion]
    - Pronate/Supinate the forearm [Twist]
3. Wrist joints :
    - Flex/Extend the wrist [Expansion]
    - Abduct/Adduct the wrist [Rotate]

Most of the major muscles are here covered in order to define their role and see if they are necessary in the model. Analysis is based on the work of Zhang [24], Kage [11], Vazquez [19], Baumel [2] and Chin [4]. The interest is first oriented toward muscles that are the strongest, as they should be those that are taking most of the effort. Thanks to the work of Yang [23], it is possible to have this list of muscles :

- Pectoralis 334 [N] PT: First there are the Pectoralis and Supracoracoideus. They are the most powerful muscles of the bird. They are recognized in the literature to be the main responsible for the beat movement of the wings. Depresses the wing.
- Supracoracoideus 108 [N] SC: Elevates the wing.
- Scapulohumeralis caudalis 50 [N] SHC: The scapulohumeralis caudalis (Teres major) is responsible for elevating and adducting the wing (Kage) .
- Coracobrachialis caudalis 32 [N] : The coracobrachialis originates on the coracoid and inserts on the humerus. It is useful to depress the wing (Kage), and given its position, could be also responsible for abducting the shoulder joint.
- Subcoracoideus 26 [N] : The subcoracoideus is similar in its attachment to the coracobrachialis; they should have the same function.
- Subscapularis 10 [N] : It is similar to the SHC, as it also originates on the scapula and inserts on the humerus.
- Rhomboideus (superficialis and profundus) 8 + 10 [N] : It is linking the spinal column to the scapula. It is not of interest here as the scapula was assumed to be fixed, and not distinguished from the rest of the main body.
- Triceps brachii humeral head 30 [N] : Linking the humerus to the ulna. It extends the elbow joint.
- Triceps brachii scapular head 20 [N] : Same as humeral head.
- Biceps brachii 26 [N] : Originates on the humerus and inserts on the radius and/or ulna (depends on the bird taxa). It flexes the elbow joint.
- Deltoideus (major + minor) 9.5 + 4 [N] : Originates on the near shoulder joint parts of the coracoid, scapula and clavicle. Rotates and abducts the wing as well as probably elevate.
- Tensor propatagialis 6 [N] : Vazquez, links elbow and manus extension.
- Extensor metacarpi radialis 19.4 [N] : Vazquez
- Flexor carpi ulnaris 25 [N] : Vazquez, links the flex of elbow and flex of the manus.
- Extensor carpi ulnaris 7.8 [N] : Vazquez, links the flex of the elbow and flex of the manus.
- Pronator superficialis + profundus 15 + 9 [N] : Responsible for twist.
- Ectepicondylo ulnaris 15 [N] : Responsible for twist
- Supinator 6 [N] : Responsible for twist
- Entepicondylo ulnaris 5.5 [N] : Responsible for twist.
- Ulnometacarpalis ventralis 3.5 [N] : Ulna + Manus : could be used
- Ulnometacarpalis dorsalis 3.2 [N] : ULna + manus : could be used.

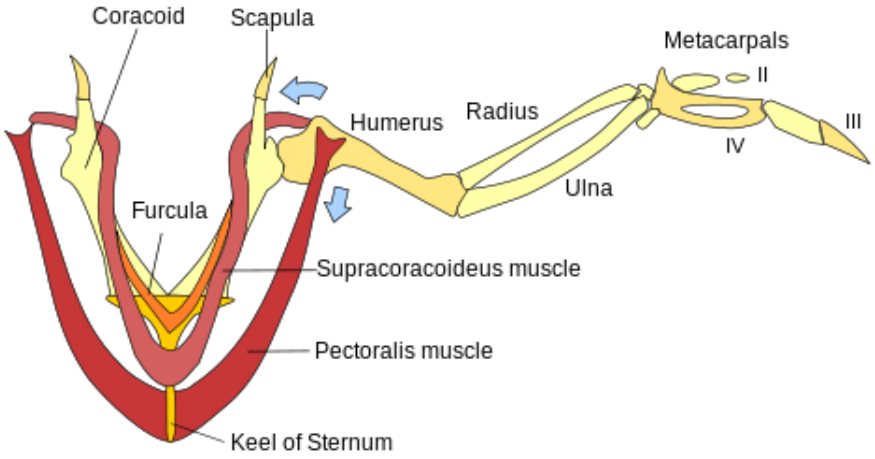

Figure 6.1 – Representation of the Supracoracoideus and Pectoralis muscles. (Figure taken from https://fr.wikipedia.org/wiki/Fichier:Wing_Muscles,_color.svg)

The final choice is to take the muscles Pectoralis (PT), with a part attached on the clavicle that we will call PTclav, Supracoracoideus (SC) and Scapulohumeralis caudalis (SHC) for the shoulder. Concerning the arm actuation, we chose the Extensor Metacarpi Radialis (EMR), Flexor carpi ulnaris (FCU), tensor propatagialis (TP) and extensor carpu ulnaris(ECU). This makes a total of 10 muscles. For now, we don't want to actuate the bird for twisting or orientation. 10 muscles are just the right amount to actuate 5 DOF, because muscles can be seen as strings that can only pull and not push. The result for all the muscle is given at Figure 6.4. All the attachments points have been scaled following the pictures to the section about attachement points.

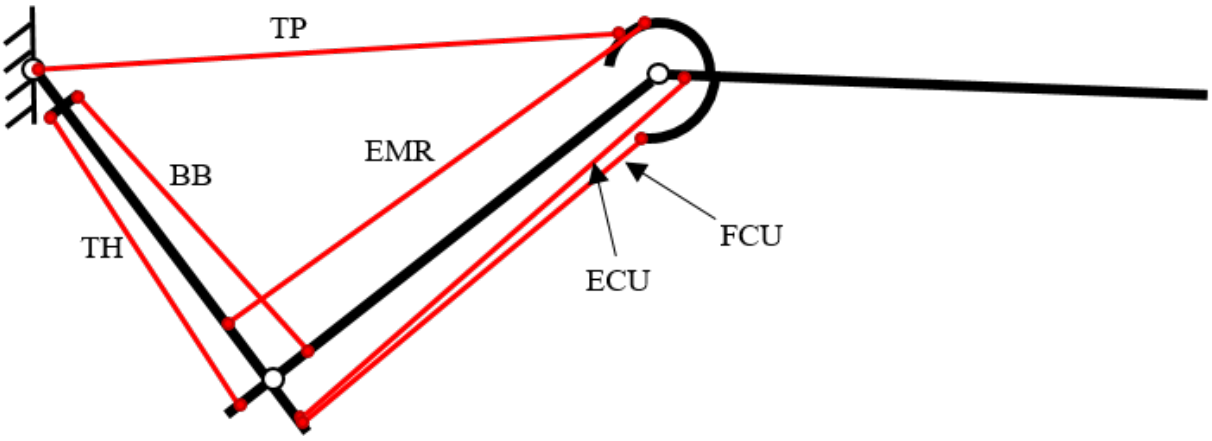

Figure 6.2 – Hill muscle model

1.1 Attachment points

All the attachement points have been represented and scaled from the following figures.

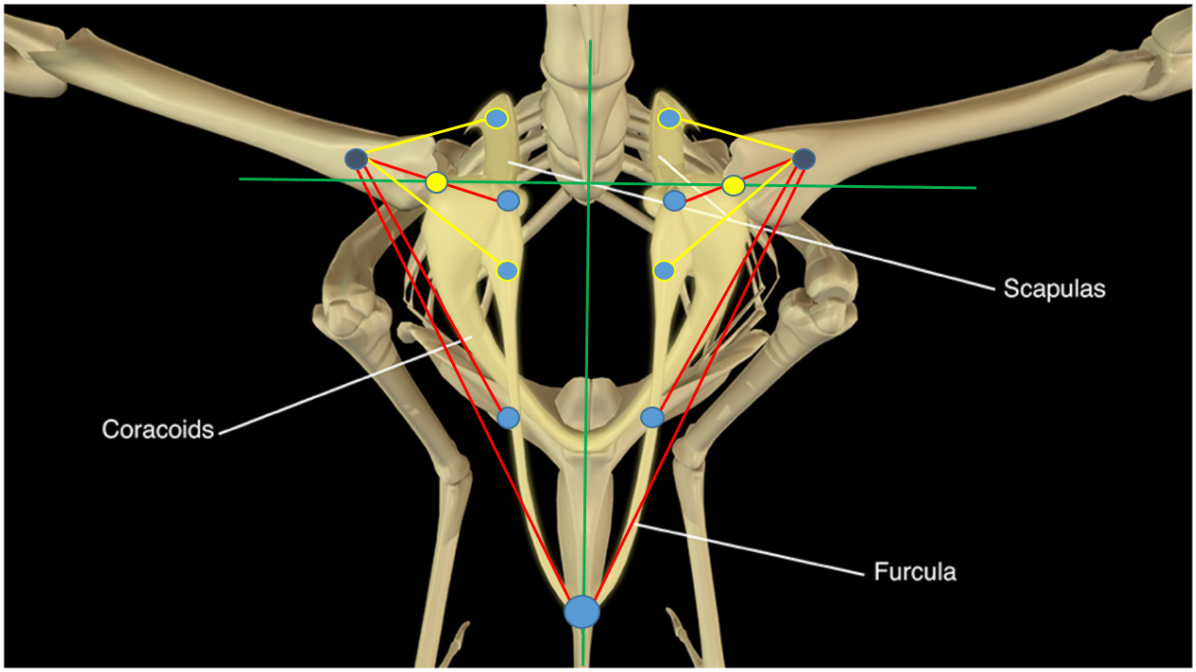

Figure 6.3 – Figure adapted from Kage [11]

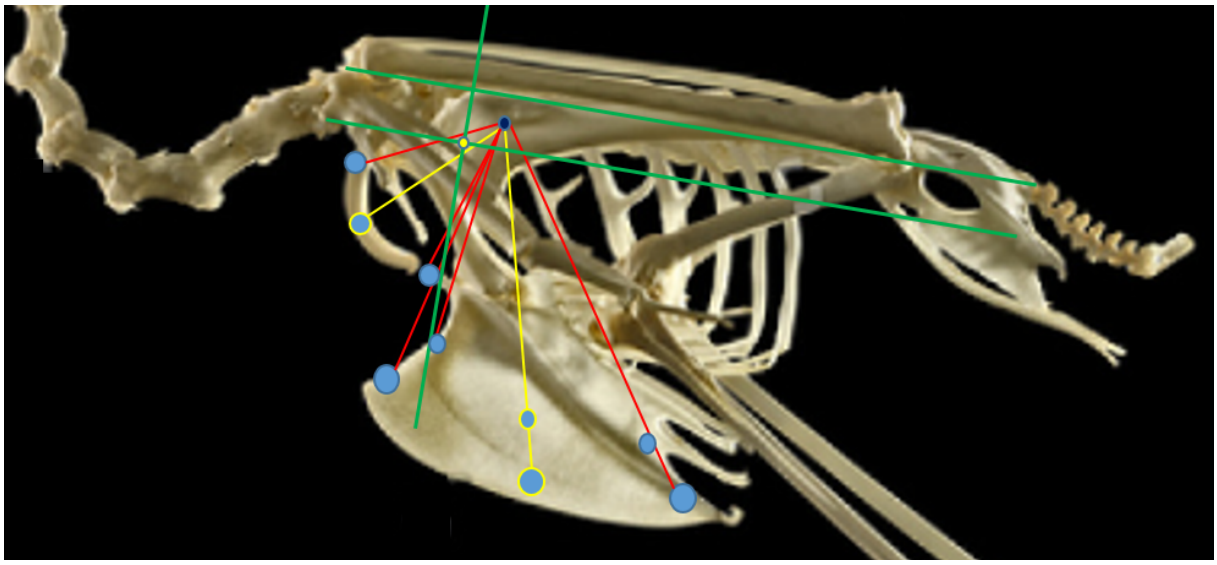

Figure 6.4 – Figure adapted from https://www.istockphoto.com/be

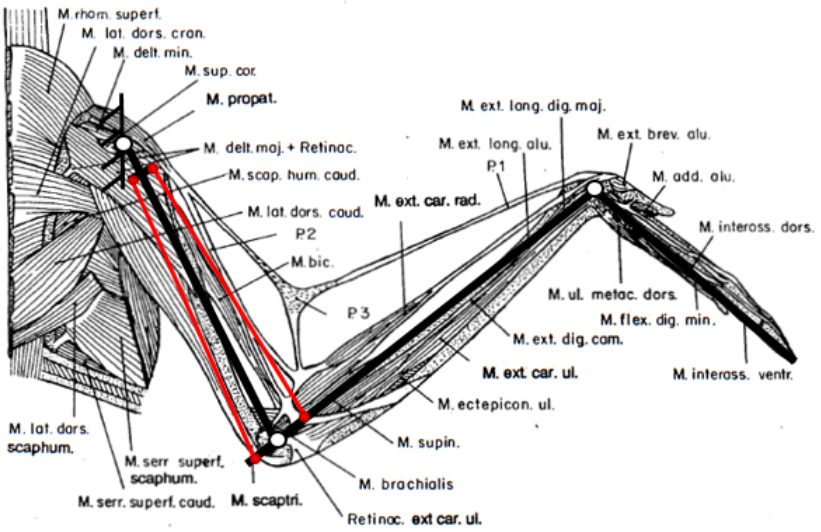

Figure 6.5 – Figure adapted from Baumel [2]

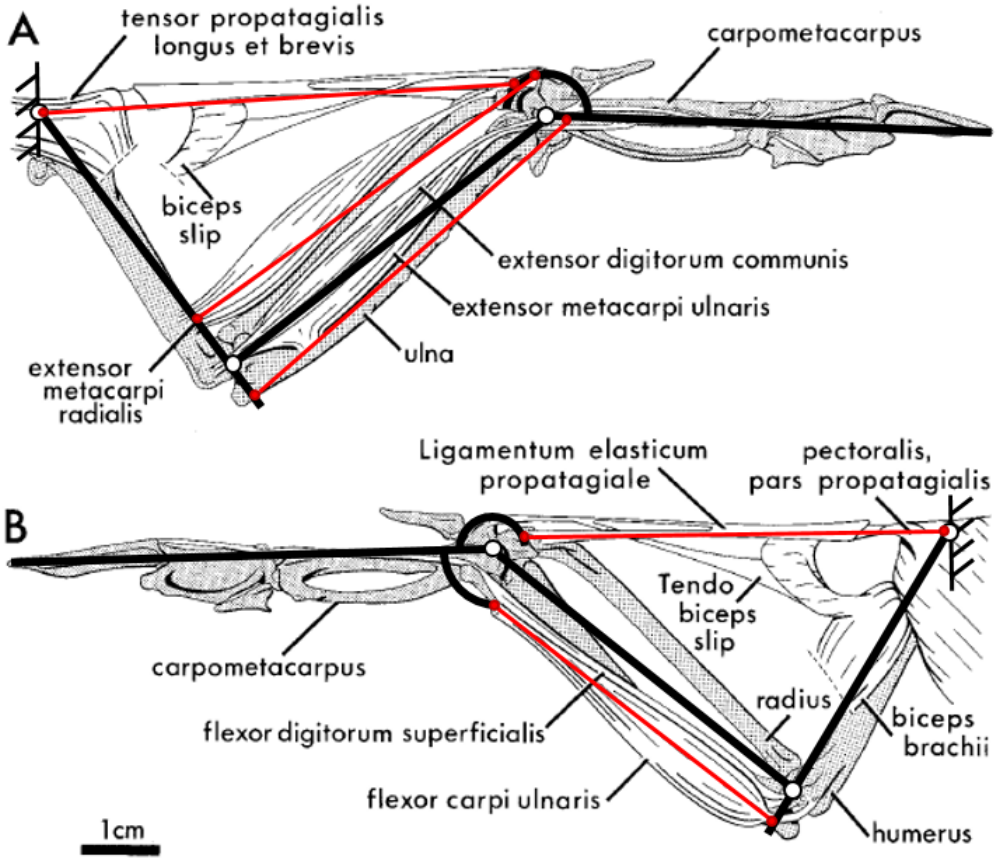

Figure 6.6 – Figure adapted from Vazquez [19]

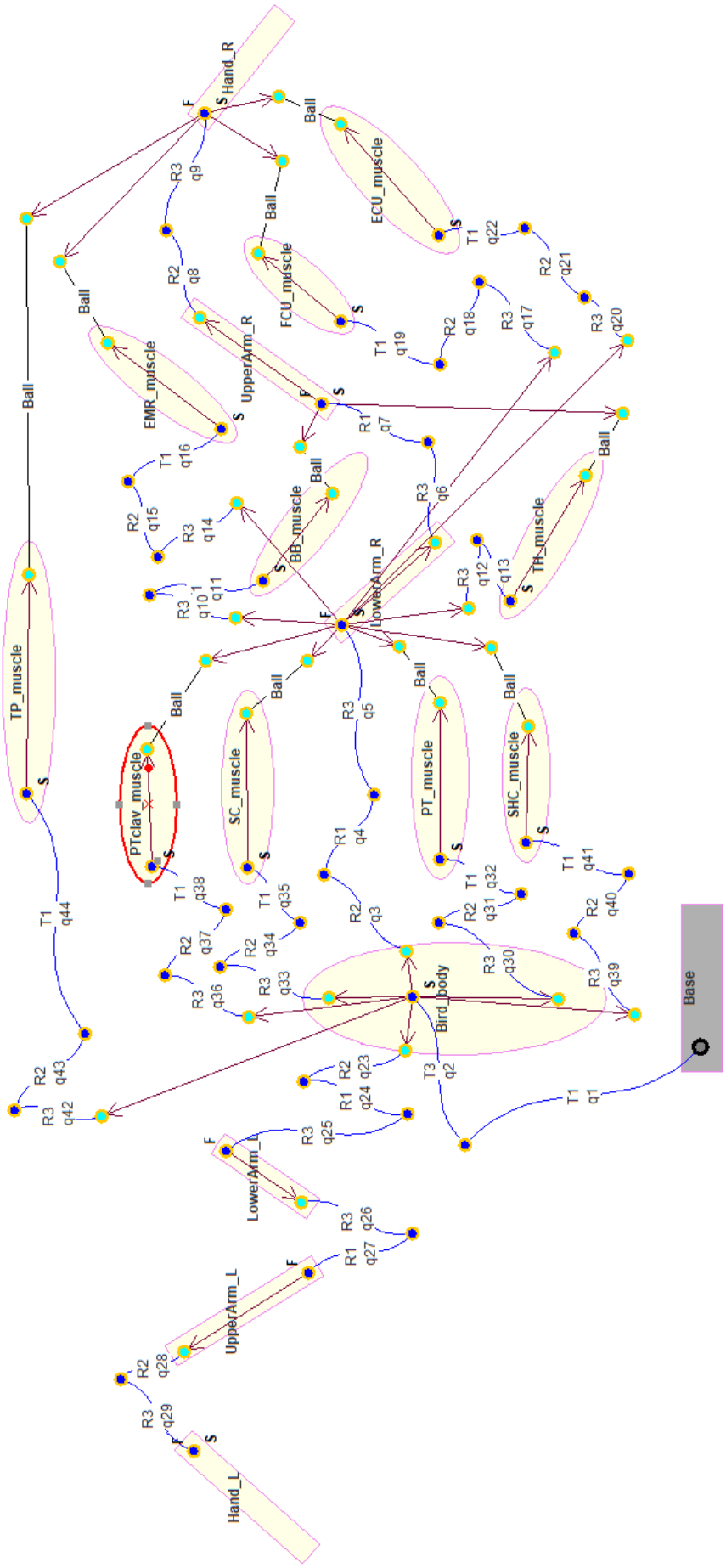

Figure 6.7 – Robotran model with muscle bodies added

2 Muscle model

2.1 Direct Hill muscle model

This section is greatly inspired from the work of Heremans [8] and Van der Noot [18] in bio-inspired actuation.

The chosen model for the muscles is the Hill model.

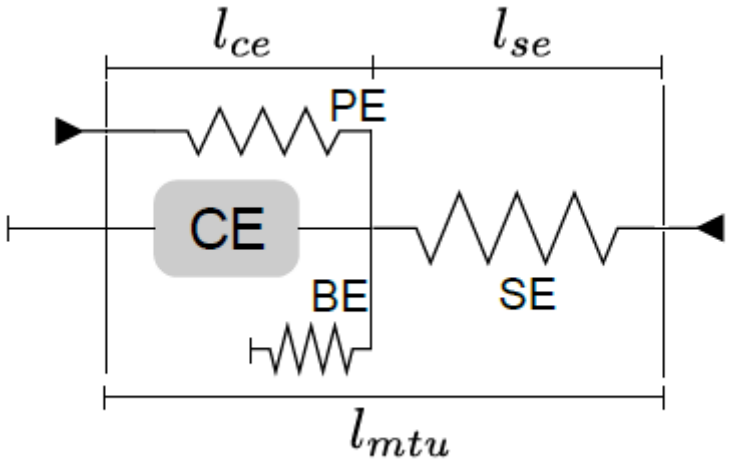

Figure 6.8 – Hill muscle model (Figure taken from Heremans [8])

First, it is important to understand the equations of the model of Hill.

They will be developed, keeping the 5 parameters that are specific to each muscles. These parameters will have to be approximated later.

$$l_{se,i} = l_{mtu,i} - l_{ce,i} \tag{6.1}$$

$$\epsilon_i = \frac{l_{se,i} - l_{slack}}{l_{slack}} \tag{6.2}$$

$$F_{se,i} = \begin{cases} \left(\frac{\epsilon_i}{\epsilon_{ref}}\right)^2 & \text{if } \epsilon_i > 0 \\ 0 & \text{else} \end{cases} \tag{6.3}$$

$$F_{se,tot,i} = F_{max} F_{se,i} \tag{6.4}$$

$$F_{be,i} = \begin{cases} F_{max} \left(\frac{l_{min} - l_{ce,i}}{l_{opt}\epsilon_{be}}\right)^2 & \text{if } l_{ce,i} \leq l_{min} \\ 0 & \text{else} \end{cases} \tag{6.5}$$

$$F^*_{pe,i} = \begin{cases} F_{max} \left(\frac{l_{ce,i} - l_{opt}}{l_{opt}\epsilon_{pe}}\right)^2 & \text{if } l_{ce,i} \leq l_{opt} \\ 0 & \text{else} \end{cases} \tag{6.6}$$

$$f_l(l_{ce,i}) = \exp\left(c \left| \frac{l_{ce,i} - l_{opt}}{l_{opt} w} \right|^3\right) \tag{6.7}$$

$$f_v(l_{ce,i}) = \frac{F_{se,i} + F_{be,i}}{A F_{max} f_l(l_{ce,i}) + F^*_{pe,i}} \tag{6.8}$$

$$F_{ce,i} = F_{se,i} + F_{be,i} - F^*{}_{pe,i} f_v(l_{ce,i}) \tag{6.9}$$

$$F_{m_i} = F_{se,i} \tag{6.10}$$

$$v_{ce,i} = \begin{cases} v_{max} \frac{1-f_v(l_{ce,i})}{1+Kf_v(l_{ce,i})} & \text{if } f_v(l_{ce,i}) < 1 \\ v_{max} \frac{f_v(l_{ce,i})-1}{7.56K(f_v(l_{ce,i})-N)+1-N} & \text{else} \end{cases} \tag{6.11}$$

Integration part : Euler integration

$$l_{ce,i+1} = l_{ce,i} + v_{ce,i}(l_{ce,i})\Delta t_i \tag{6.12}$$

The parameters of the model (taken from Geyer [7]):
$w = 0.56 | \epsilon_{ref} = 0.04 | \epsilon_{be} = \frac{w}{2} | \epsilon_{pe} = w | c = \ln 0.05 | K = 5 | N = 1.5$
$f_{l,inf} = 0.001$, $f_{v,inf} = 0$ and $f_{v,sup} = 1.5$.

2.2 Inverting the muscular model

To inverse the model, the equations must be taken in inverse path. From the instantaneous torques in all the joints of both wings, the goal is to retrieve the necessary pattern of activation of A_m in each muscle. Given this result, it will be possible to compare it with EMG signals from other authors.

First of all, it is needed to extract the linear forces in each muscle in order to invert the Hill muscle model. However, there are more muscles than joints to activate so that it is a problem of over-actuation that has to be solved. The process of solving this problem is dedicated to Section 2.3. Once the over-actuation has been solved, the Hill model can be inverted from the forces F_m, i in the muscles. The inverted set of equations is as follows :

$$F_{se,i} = F_{m,i} \tag{6.13}$$

$$l_{se,i} = \epsilon_{ref} l_{slack} \sqrt{\frac{F_{se,i}}{F_{max}}} + l_{slack} \tag{6.14}$$

$$l_{ce,i} = l_{mtu,i} - l_{se,i} \tag{6.15}$$

We use finite differences equations to derive $l_{ce,i}$ and obtain $v_{ce,i}$.

$$v_{ce}[k] = \left[-\frac{1}{3} l_{ce}[k-3] + \frac{3}{2} l_{ce}[k-2] - 3 l_{ce}[k-1] + \frac{11}{6} l_{ce}[k] \right] \left(\frac{1}{\Delta t} \right) \tag{6.16}$$

Afterwards, the internal forces are computed. The three following equations are the same as in the direct model.

$$F_{be,i} = \begin{cases} F_{max} \left(\frac{l_{min} - l_{ce,i}}{l_{opt} \epsilon_{be}} \right)^2 & \text{if } l_{ce,i} \leq l_{min} \\ 0 & \text{else} \end{cases} \tag{6.17}$$

$$F^*{}_{pe,i} = \begin{cases} F_{max} \left(\frac{l_{ce,i} - l_{opt}}{l_{opt} \epsilon_{pe}} \right)^2 & \text{if } l_{ce,i} \leq l_{opt} \\ 0 & \text{else} \end{cases} \tag{6.18}$$

$$f_l(l_{ce,i}) = \exp \left(c \left| \frac{l_{ce,i} - l_{opt}}{l_{opt} w} \right|^3 \right) \tag{6.19}$$

As regards f_v the equation is different.

$$f_v(v_{ce,i}) = \begin{cases} \frac{v_{max} - v_{ce,i}}{K v_{ce,i} + v_{max}} & \text{if } v_{ce,i} < 0 \\ \frac{v_{ce,i}[(7.56K+1)N-1] - v_{max}}{v_{ce,i} 7.56K - v_{max}} & \text{else} \end{cases} \tag{6.20}$$

$$F_{ce,i} = F_{se,i} + F_{be,i} - F_{pe,i}{}^* f_l(l_{ce,i}) \tag{6.21}$$

$$A_m = \frac{F_{ce,i}}{F_{max} f_l f_v} \tag{6.22}$$

where A_m is the activation signal that should be applied to the muscle to produce the same force.

2.3 Over-actuation problem and optimization

The whole problem of the over-actuation is that there are 7 DOF for each wing, but 10 muscles. The general problem is the equation of torques.

$$\underline{\tau} = \underline{\underline{R}} \cdot \underline{F} \tag{6.23}$$

where $\underline{\tau} \in \mathbb{R}^{7\times1}$, $\underline{\underline{R}} \in \mathbb{R}^{7\times X}$ and $\underline{F} \in \mathbb{R}^{X\times1}$.

Note that the muscles forces can only be positive, as muscles can be seen as cables for actuation. They can only pull by contraction and not push on the bodies.

As visible on Equation 6.23, the problem is a linear system of 7 equations and 14+ equations. The system is thus under-constrained and an added criterion is needed. The choice is to make an optimization similar to what muscles do in reality. Forces are going to be pondered depending on the maximal force F_{max} that the muscle can generate. It means that stronger muscles are going to take more of the load compare to weaker muscles.

It is a problem of linear optimization stated as follows :

$$\min \sum_{i=1}^{7} \alpha_i |F_i| = \min \sum_{i=1}^{7} \alpha_i F_i \text{ with } F_i^{max} \geq F_i \geq 0 \ (i = 1 \dots 7),\ \underline{\tau} = \underline{\underline{R}} \cdot \underline{F} \tag{6.24}$$

In the problem, α_i are chosen as $\alpha_i = \frac{1}{F_i^{max}}$. The problem can be solved by an algorithm of linear programming. Solving this problem is equivalent to finding the set of forces that best share the loads among the muscles depending on their strength. The problem here is solved using `linprog` from the optimization library of MATLAB.

Nonetheless, to be able to solve the general problem, one needs to assemble the $\underline{\underline{R}}$ matrix.

The problem can be reformulated. It would be useful as formulation to express each lever arm, i.e. each component of the matrix $\underline{\underline{R}}$, in the reference frame i of the joint torque necessary in joint i.

For each joint j, the following equation can be written :

$${}^j\underline{\tau} = \sum_i {}^j\underline{r}_{om,i} \times {}^j\underline{F}_{m,i} \tag{6.25}$$

In the problem, Robotran is able to give certain values. The values available are : $Q_{q,i}$, ${}^{bk}\underline{r}_{om,i}$, ${}^{mi}\underline{F}_{m,i}$, ${}^I_i\underline{\underline{R}}$, ${}^I_{bk}\underline{\underline{R}}$ and ${}^I_{mi}\underline{\underline{R}}$, where I is the inertial frame, mi, bk and j are respectively indices of the frames of muscle i, bone k and joint j. The problem can be rewritten as,

$${}^j\underline{\tau} = \sum_i \left({}^j_{bk}\underline{\underline{R}}\ {}^{bk}\underline{r}_{om,i}\right) \times \left({}^j_{mi}\underline{\underline{R}}\ {}^{mi}\underline{F}_{m,i}\right) \tag{6.26}$$

$${}^j\underline{\tau} = \sum_i \left({}^j_I\underline{\underline{R}}\ {}^I_{bk}\underline{\underline{R}}\ {}^{bk}\underline{r}_{om,i}\right) \times \left({}^j_I\underline{\underline{R}}\ {}^I_{mi}\underline{\underline{R}}\ {}^{mi}\underline{F}_{m,i}\right) \tag{6.27}$$

$$ {}^{j}\underline{\tau} = \sum_{i} \left(\left({}^{I}_{j}\underline{\underline{R}} \right)^{T} \; {}^{I}_{bk}\underline{\underline{R}} \; {}^{bk}\underline{r}_{om,i} \right) \times \left(\left({}^{I}_{j}\underline{\underline{R}} \right)^{T} \; {}^{I}_{mi}\underline{\underline{R}} \; {}^{mi}\underline{F}_{m,i} \right) \tag{6.28} $$

$$ {}^{j}\underline{\tau} = \sum_{i} tilde \left(\left({}^{I}_{j}\underline{\underline{R}} \right)^{T} \; {}^{I}_{bk}\underline{\underline{R}} \; {}^{bk}\underline{r}_{om,i} \right) \left({}^{I}_{j}\underline{\underline{R}} \right)^{T} \; {}^{I}_{mi}\underline{\underline{R}} \; {}^{mi}\underline{F}_{m,i} \tag{6.29} $$

Knowing that $F_{m,i}$ and $Q_{q,j}$ are respectively components of ${}^{mi}\underline{F}_{m,i}$ and ${}^{j}\underline{\tau}$, the only remaining element is to take the right component of the matrix $\underline{\underline{M}} \in \mathbb{R}^{3\times3}$ and put it at its place in $\underline{\underline{R}}$. M is defined as :

$$ \underline{\underline{M}} = tilde \left(\left({}^{I}_{j}\underline{\underline{R}} \right)^{T} \; {}^{I}_{bk}\underline{\underline{R}} \; {}^{bk}\underline{r}_{om,i} \right) \left({}^{I}_{j}\underline{\underline{R}} \right)^{T} \; {}^{I}_{mi}\underline{\underline{R}} $$

This matrix $\underline{\underline{M}}$ must be computed for each muscle that has an influence on each joint.

3 Parameters identification for muscles

This section focuses on the identification of the parameters for the muscles. Now that the problem of muscular actuation has been solved in the general way, the model must be tuned to be able to actuate the wings in a consistent way. For each muscle, the following set of parameters must be defined : l_{opt}, l_{opt}, l_{slack}, l_{min}, v_{max} and f_{max}.

First, it is important to note that the model of actuation is an approximation. It means that all the real muscles of the bird will not be represented. This choice is motivated by the large number of muscles. Some criteria are necessary to choose just the most important muscles.

On Table **??**, the exhaustive amount of muscles is numbered. Note that all the development is based on data obtained from a Gold Pheasant, as it is the only available. The stronger muscles are chosen in first place.

4 Comparison with real measurements

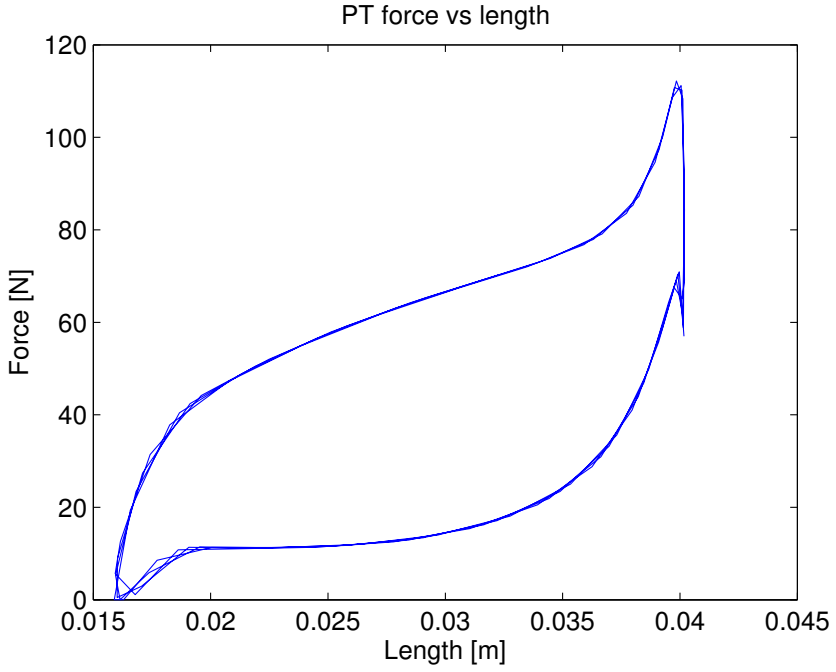

Figure 6.9 – Force of the Pectoralis in function of the muscle length

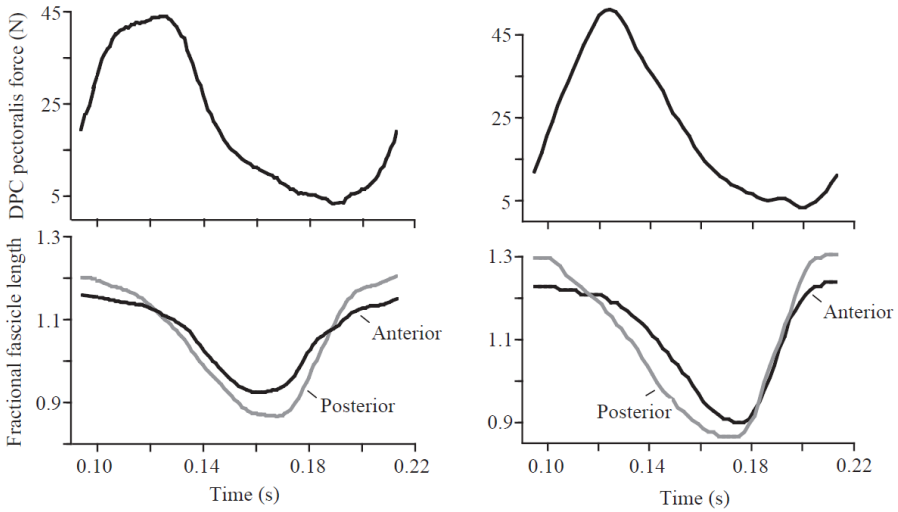

Figure 6.10 – Force of the Pectoralis (anterior and posterior) compared to fascicle length (Figure taken from Biewener [3])

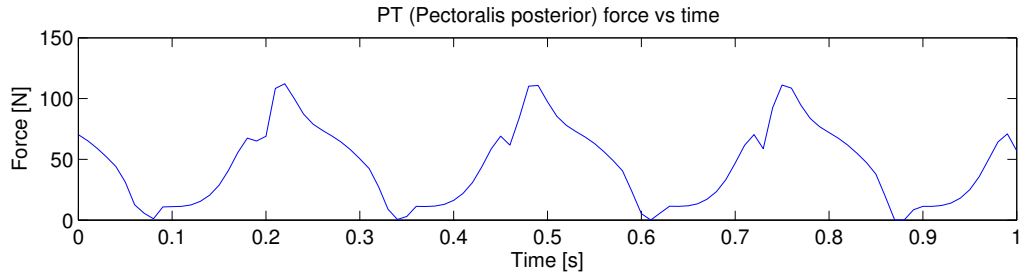

(a)

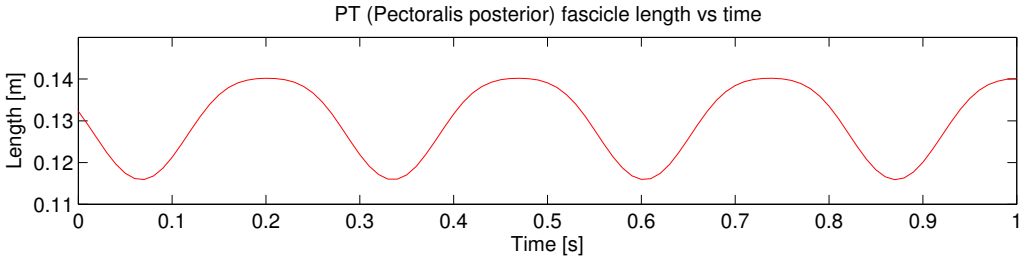

(b)

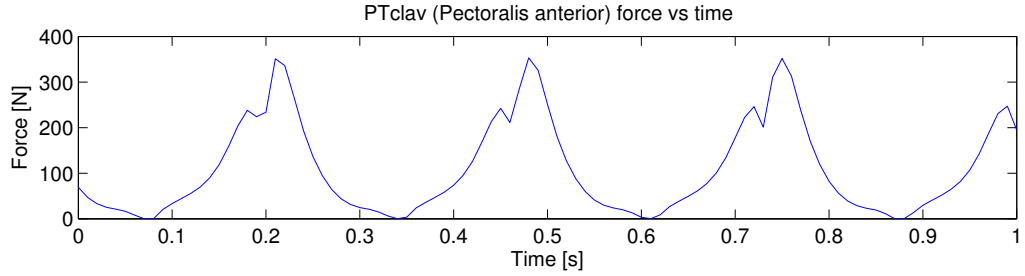

(c)

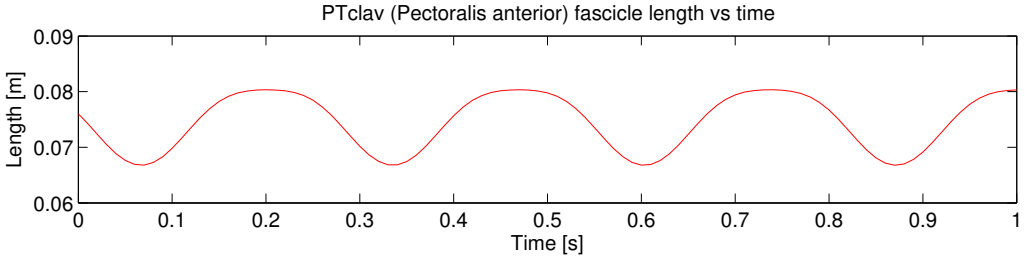

(d)

Figure 6.11 – Pectoralis anterior (clavicle) and posterior (keel) parts compared to fascicle lengths.

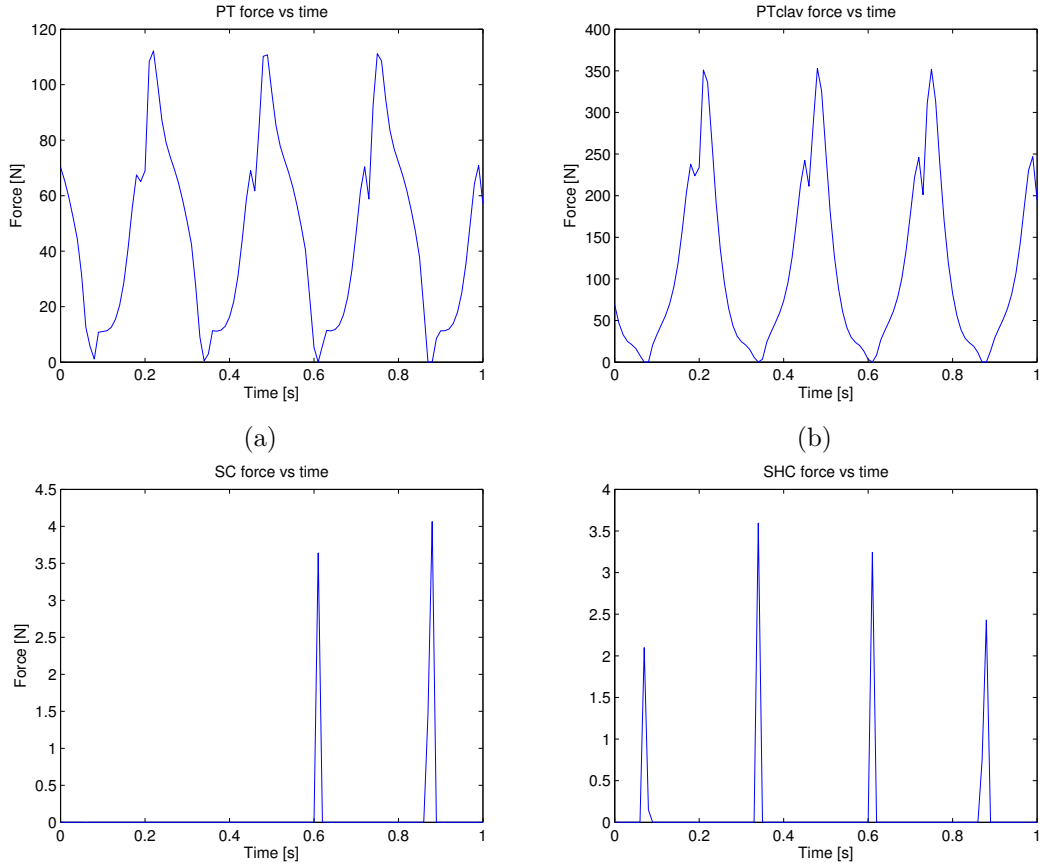

Figure 6.12 – Shoulder muscles forces in function of time

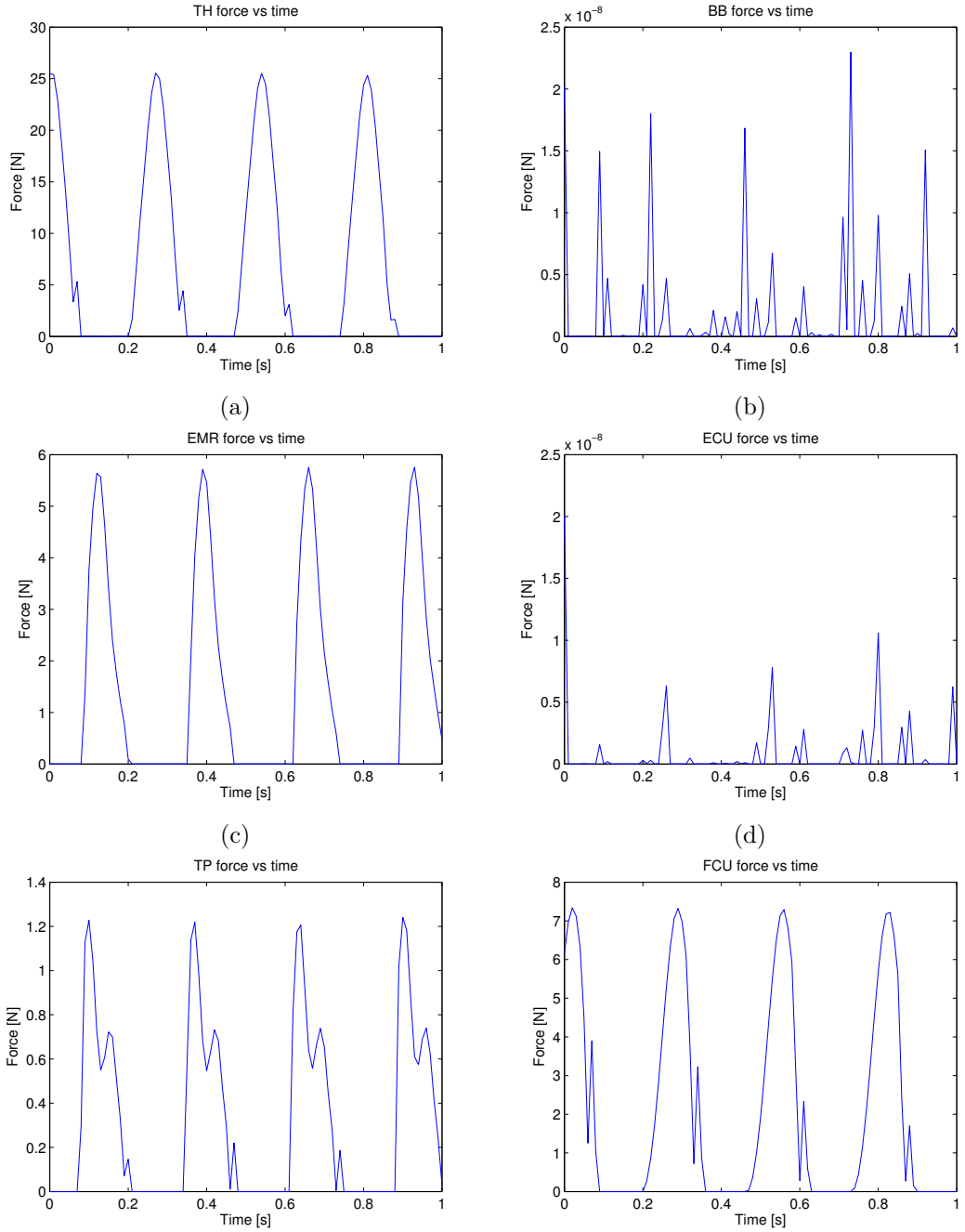

Figure 6.13 – Wing morphing muscles forces in function of time

Chapter 7

Take-aways and perspectives

1 Summary of Results - Conclusion

The thesis comes now at an end. It is now interesting to look back at the work achieved, the results obtained and have a critical analysis of it.

A good result is that the bird is already able to fly. This was made possible by a good composition of the multibody mechanical system, the aerodynamic model and a good scaling. It was also necessary to analyze the kinematics available from Geronticus Eremita. However, the mechanical model has still 2 DOF only for the bird body which is still few.

Concerning the aerodynamic model, the values of coefficients of drag and lift came from plane profile. As it is obviously not the case here, the result should still be taken cautiously. One way could be to check in the literature for measured coefficients for bird wings.

The results obtained from extrapolation of measures from other birds seem quite realistic. The data is still pretty close to the measures of other ibis, birds that should have the same kind of morphology as the Geronticus Eremita, as they are all members of the Threskiornithidae family gathering all ibis and spoonbils.

The kinematics made the fligt of the bird possible, which is a great result. Even tough multiple assumptions wer needed, plotting the approximation against the data made us realize that the result stays quite close to the measures.

Sadly, it was not yet possible to extract good parameters for the muscle models. Therefore, even though the muscle models are already coded in the simulator, they have not been validated. Nevertheless, the general problem of overactuation has been solved for muscle in 3 dimensions. This allows now for an easy manipulation of muscles. More can be added if wanted, all functionnal. Yet, the results of forces obtained can hardly be more validated if no more data is available. Finally, the results for the attachment points for the current chosen muscles should be relatively precise. However, they could be more precise if more data for these special features were found.

2 Future perspectives

Even tough the analysis is now ended, it is interesting to realize all the work still to come to reach the final goal of the Project RevealFlight. Here are multiple areas of the project that still have room for improvement.

Mechanical model

The mechanical model obtained at the end of the thesis, in the multibody point of view, is already a quite complex model. The number of DOF is already quite large and should be able to simulate any bird. However, in future work, it would be necessary to free all the other DOF of the bird's body. As a reminder, it was only allowed 2 DOF in translation. This is the possible

reason why the model is stable in open loop. In order to fly with all the DOF freed, it will also be necessary to implement a tail to the bird and add its own aerodynamic model.

Aerodynamic model

The aerodynamic model currently implemented is quite simple and should be upgraded. As the purpose of the RevealFlight project is to analyze the interactions in flock of birds, a large computational fluids simulation should be added. This model should take into account the complex turbulence effects created by the wakes of the wing beats and their advantages in formation flight. Moreover, the wing cut in segments should be replaced. As it is already done by other authors, all the feathers should be represented separately. This is an unavoidable step in order to access to a higher order of precision of aerodynamics interactions bird - fluid. A few more general aspects are that a aerodynamic tail should be added to prevent the bird from desequilibrium once the pitch axis rotation is freed. Finally, the bird body should also be visible on the aerodynamic point of view, to represent the amount of drag generated. That would potentially change the dynamic of flight.

Scaling of the Geronticus Eremita

Concerning the scaling of the Geronticus, the analysis has already been quite extensive. All the lengths of interest have been covered. However, it is important to notice that not a really large amount of data was available. Especially for the aeordynamic parameters WS, WA and AR, the values are possibly biased by a lack of measures. Luckily, there are still unused data from Pennycuick [13], also from the order of ciconiiformes and ardeidae that has still to be added to have a more solid sample. Obvioulsy, if a Geronticus Eremita was at hand, it would be probably directly possible to measure most of the needed values.

Kinematics of flight

The kinematics of the bird flight have been studied with the data available. However, it is important to remind ourselves that multiple assumptions have been made. The elbow and shoulder expansion DOF were approximated to constants, the twisting of the elbow for supination/pronation was considered to be zero. Even though these assumptions were "good enough" and allowed the bird to fly, they have possibly an impact on fine tuning of the flight. One way for solving that would have to finf better data. Another way would be to forget the data and choose an approach similar to Shim [14], where the parameters of flight are found by evolutionary algorithms. The purpose would then be to optimize the flight following a criteria.

Another aspect is that the bird is still currently flying in open loop. In the future, one should find a way to add feedback in order to avoid drift in speed and height. Moreover, a feedback controller will probably be essential when the other DOF of the bird body will be freed.

Muscle model

There is still a lot of work to do concerning the muscles. This is probably the aspect that should be the main focus in future work. As it was not possible to already find the muscle parameters, it is a step unavoidable of future work because the muscle model is at the center of the link between muscle recordings and kinematics. It is needed for RevealFlight. As there is no method to finf them right now, some research will be needed. One way could be to also use evolutionary algorithms on the muscle parameter and find the right criteria to optimize. Once the muscle models are ready, it will be possbile to create the "neuro" block that will generate the activation patterns : it is the next step. A CPG would be probably a good choice. Finally, an interesting topic would be to link aerodynamic model composed of feathers, with the muscles models, as it

is the case for the real bird. The feathers can be oriented by the muscles and have some relative degrees of freedom with the skeleton.

Bibliography

[1] Douglas L. Altshuler, Joseph W. Bahlman, Roslyn Dakin, Andrea H. Gaede, Benjamin Goller, David Lentink, Paolo S. Segre, and Dimitri A. Skandalis. The biophysics of bird flight: functional relationships integrate aerodynamics, morphology, kinematics, muscles, and sensors. *Canadian Journal of Zoology*, 93(12):961–975, 2015.

[2] Julian J. Baumel, editor. *Handbook of Avian Anatomy : Nomina Anatomica Avium, Second Edition*. Publications of the Nuttall Ornithological Club, No 23, Cambridge, Massachusetts, 1993.

[3] A. A. Biewener, W. R. Corning, and B. W. Tobalske. In vivo pectoralis muscle force-length behavior during level flight in pigeons (columba livia). *Journal of Experimental Biology*, 201(24):3293–3307, 1998.

[4] Diana D. Chin, Laura Y. Matloff, Amanda Kay Stowers, Emily R. Tucci, and David Lentink. Inspiration for wing design: how forelimb specialization enables active flight in modern vertebrates. *Journal of The Royal Society Interface*, 14(131), 2017.

[5] John B. Dunning, Jr., editor. *CRC Handbook of Avian Body Masses, Second Edition*. CRC Press, 2008.

[6] D. J. Field, C. Lynner, C. Brown, and Darroch S. A. F. Skeletal correlates for body mass estimation in modern and fossil flying birds. *PLoS ONE*, 8(11), 2013.

[7] Hartmut Geyer and Hugh Herr. A muscle-reflex model that encodes principles of legged mechanics produces human walking dynamics and muscle activities. *IEEE Transactions on Neural Systems and Rehabilitation Engineering*, 18(3), 2010.

[8] François Heremans. Controlling the balance of a humanoid robot subject to large perturbations. Master's thesis, Université Catholique de Louvain, 2015.

[9] Tobin L. Hieronymus. Flight feather attachment in rock pigeons (columba livia): covert feathers and smooth muscle coordinate a morphing wing. *Journal of Anatomy*, 229(5):631–656, 2016.

[10] Eunjung Ju, Jungdam Won, Jehee Lee, Byungkuk Choi, Junyong Noh, and Min Gyu Choi. Data-driven control of flapping flight. *ACM Trans. Graph.*, 32(5):151:1–151:12, October 2013.

[11] Kelly M. Kage. *A Portrayal of Biomechanics in Avian Flight*. PhD thesis, Rochester Institute of Technology, 2014.

[12] Irby J. Lovette and John W. Fitzpatrick, editors. *Cornell Lab of Ornithology's handbook of bird biology*. John Wiley & Sons, 2016.

[13] C.J Pennycuick. *Modelling the Flying Bird*. Elsevier Inc., 2008.

[14] Yoon-Sik Shim and Chang-Hun Kim. Evolving physically simulated flying creatures for efficient cruising. *Artif. Life*, 12(4):561–591, October 2006.

[15] YoonSik Shim and Phil Husbands. Feathered flyer: Integrating morphological computation and sensory reflexes into a physically simulated flapping-wing robot for robust flight manoeuvre. In Fernando Almeida e Costa, Luis Mateus Rocha, Ernesto Costa, Inman Harvey, and António Coutinho, editors, *Advances in Artificial Life*, pages 756–765, Berlin, Heidelberg, 2007. Springer Berlin Heidelberg.

[16] Erin L.R. Simons. Forelimb skeletal morphology and flight mode evolution in pelecaniform birds. *Zoology*, 113(1):39 – 46, 2010.

[17] B Tobalske and K Dial. Flight kinematics of black-billed magpies and pigeons over a wide range of speeds. *Journal of Experimental Biology*, 199(2):263–280, 1996.

[18] Nicolas Van der Noot. *Rich and Robust Bio-Inspired Locomotion Control for Humanoid Robots*. PhD thesis, École Polytechnique Fédérale de Lausanne & Université Catholique de Louvain, 2017.

[19] R. J. Vazquez. The automating skeletal and muscular mechanisms of the avian wing (aves). *Zoomorphology*, 114(1):59–71, Mar 1994.

[20] X Wang, AJ McGowan, and GJ Dyke. Avian wing proportions and flight styles: First step towards predicting the flight modes of mesozoic birds. *PLoS ONE*, 6(12), 2011.

[21] Bird flight. https://en.wikipedia.org/wiki/Bird_flight. Accessed: 2018-07-01.

[22] Jia-chi Wu and Zoran Popović. Realistic modeling of bird flight animations. *ACM Trans. Graph.*, 22(3):888–895, July 2003.

[23] Yan Yang, Huan Wang, and Zihui Zhang. Muscle architecture of the forelimb of the golden pheasant (chrysolophus pictus) (aves: Phasianidae) and its implications for functional capacity in flight. *Avian Research*, 6(1):3, Mar 2015.

[24] Z. Zhang and Y. Yang. Forelimb myology of the golden pheasant (chrysolophus pictus). *Int. J. Morphol.*, 31(4):1482–1490, 2013.

Appendix

Rue Archimède, 1 bte L6.11.01, 1348 Louvain-la-Neuve **www.uclouvain.be/epl**